14A.8

# EQUILIBRIUM TRANSLATION MODEL – A KEY TO PREDICTION OF TROPICAL HURRICANE INTENSITY

Irakli G. Shekriladze*
Georgian Technical University, Tbilisi, Georgia

## 1. INTRODUCTION

As it is commonly accepted generation and development of tropical hurricane (TH) depends from the following three key conditions: wide area with sea-surface temperature (SST) more than 26 $^0$C, environmental wind with low vertical shear and the Coriolis parameter sufficient for vorticity generation (Palmen and Newton 1969, Emanuel 1999, Goldenberg et al. 2001). Below it is shown that additionally certain type of conformity between dynamical and thermal environmental fields also is decisive, specifically, through rapid intensification of the most powerful hurricanes.

The spectrum of characteristic scales of tropical hurricane (TH) begins with sprayed by wind water droplet and ends by comparable to the planetary sizes inflowing atmospheric currents. Description of such a complex phenomenon requires accounting of great variety of interrelated irreversible thermo-hydrodynamic processes. That is why numerical methods of modeling in combination with wide field observations become main instrument of TH research during last decades. By now this "numerical" attack is in progress with certain achievements, for instance, in TH track forecasting (Webber 2005a).

At the same time the problem of forecasting of rapid changes of TH intensity still remains as the most critical (Krishnamurti et al. 2005, Webber 2005). According to review of forecast advisories (UNISYS Weather: Hurricane/Tropical Data/Archive) during 2004-2005 regular predictions have overlooked or significantly underestimated practically all cases of rapid intensification.

Pressing character of the problem is reflected also by wide front of research of potential mechanisms of TH intensification (Emanuel 2004, Zhu et al. 2004, Wu and Braun 2004, Persing and Montgomery 2005, Lin et al. 2005, Shapiro and Moller 2005, Corbosiero et al. 2005, Wu et al. 2005, Möller and Shapiro 2005). High emphasis is placed also on vital problem of clarification of potential influence of global warming on TH intensity (Trenberth 2005, Kerr 2005, Emanuel 2005).

Aforementioned principal challenges highlight pressing contemporary problem of proper combination of numerical methods with adequate qualitative physical models.

In certain degree this gap is bridged by equilibrium translation model (ETM) (Shekriladze 2004a). ETM links rapid development of tropical hurricane to conformity of dynamical and thermal environmental fields. According ETM TH achieves peak efficiency in conversion of ocean heat potential into cyclonic motion of atmosphere when its translation is found to be in certain accordance with intensity of heat removal from ocean upper layer (alignment effect).

In the framework of ETM the role of the main characteristic of TH development is gained by non-dimensional alignment number incorporating main thermal and dynamical parameters of the system TH-ocean. Alignment number, representing a measure of conformity dynamical and thermal fields, by its part ultimately directly is linked to so-called heat involvement factor.

Fundamental character of the effect is confirmed by wide field data on the cases of rapid intensification observed in 2004-2005 (including tropical hurricanes Charley, Katrina and Wilma). Potential is created for qualitative improvement of tropical hurricane intensity prediction

## 2. EQUILIBRIUM TRANSLATION MODEL

Certain initial conformity of dynamical and thermal environmental fields almost always holds in the zones of a TH development. It is caused

• *Corresponding author address:* Irakli G. Shekriladze, Georgian Technical Univ., 77 Kostava Street, Tbilisi, 0175, Georgia; e-mail: shekri@geo.net.ge

by formation of background SST field by background dynamical field itself. In main zones of TH development direction of background SST elevation, as a rule, coincides with environmental wind. In trade winds zone SST elevation rate is of order of $10^{-6}$ $^0$C m$^{-1}$ (McGraw-Hill Encyclopedia of Ocean and Atmospheric Sciences 1980).

Another level of conformity of environmental fields is formed by longitudinal SST jump induced by TH itself. TH translation necessarily leads to considerable lowering of SST on its rear. The resultant SST jump forms local SST elevation rate of order of $10^{-5}$ $^0$C m$^{-1}$. In this connection the influence of SST jump mentioned assumes prevailing significance.

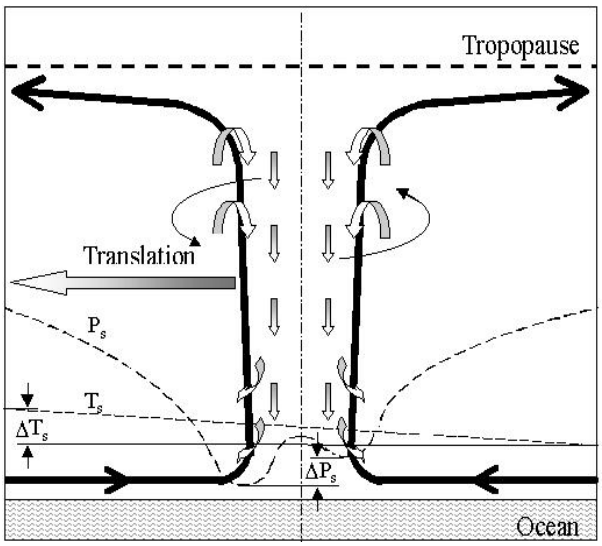


Fig. 1. Scheme of TH thermal driving mechanism.

Interaction of environmental fields may be considered based at the scheme of TH thermal driving mechanism presented in the Fig. 1.

SST jump ($\Delta T_s$) caused by asymmetry of energy inflow in TH leads to more intense ascending flow in frontal part of the eye wall cloud with corresponding minimum of air pressure. Generated by thermal asymmetry pressure drop between frontal and back parts of the eye wall cloud ($\Delta P_s$) just creates driving force.

Intensity of heat and mass transfer from a sea surface to TH is little affected by translation speed. Here main role is played by much higher air tangent velocity (for instance, beginning from outer boundary with tangent velocity 15 ms$^{-1}$). In this connection reduction of translation speed (leading to prolonging of TH passage above given area of a sea surface) steps up the share of heat removed from upper ocean layer, and vice versa, gathering of translation reduces cooling of the layer mentioned, all other things being the same.

Inverse dependence mentioned introduces rather strong feedback into thermal driving mechanism. Reduction of translation speed, alongside with increasing $\Delta T_s$, leads to elevation of pressure drop $\Delta P_s$ causing, for its part, TH acceleration.

In such a manner, TH not only prefers to shift toward SST elevation direction, but it also tends to establish certain equilibrium between translation speed and integral heat flux.

Generation of thermal driving force depends from TH translation speed and hurricane thermal potential (HHP) (Leipper and Volgenau 1972) of given area. Besides, generation of the same driving force needs more slow translation of TH at high value of HHP and vice-versa. This inverse dependence roughly corresponds to constancy of heat involvement factor (equal to the share of HHP removed by TH from an ocean through passage of given area) during equilibrium translation. The last supposition is supported by analysis of the field data on TH Opal (1995) presented in Fig. 2.

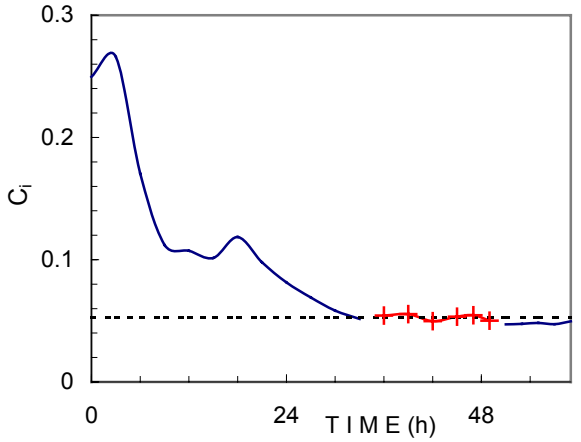


Fig. 2. Variation of heat involvement factor ($C_i$) during development of TH Opal (1995): crosses – TH rapid intensification stage.

At the same time establishment of equilibrium translation is possible only through it's favoring by dynamical field. ETM assumes that Just conformity of dynamical and thermal fields triggers intensive TH development (alignment effect).

### 2.1 The First Approximation

Realization of ETM in the first approximation (FAP) (Shekriladze 2004a) is built upon

consideration of uniform straightforward translation of circular TH. Within accepted assumptions heat balance of an ocean upper layer inside an area with leading role of tangent winds in heat removal from a sea surface is determined in following form:

$$2C_i Q R_{15}\left(U_{tr} - U_{dr} - C_\varphi \frac{dR_{15}}{d\tau}\right) = \pi R_{15}^2 q \quad (1)$$

Here $C_i$ is heat involvement factor; Q is averaged inside $R_{15}$ HHP; $R_{15}$ is radius of a TH at tangent velocity 15 m $s^{-1}$; q is averaged inside $R_{15}$ integral (sensitive and latent) heat flow from sea surface to TH; $U_{dr}$ is component of sea surface drift speed parallel to translation; $\tau$ is time.

Assuming in addition insignificancy of a sea surface drift, relationship between main dynamical and thermal parameters of combined ocean-atmosphere system during equilibrium translation (to say, at the stage of TH intensification) is reduced to following equation for non-dimensional alignment number:

$$N_{al} = \frac{U_{tr} Q}{q R_{15}} = 25 \quad (2)$$

For TH holding roughly constant size and other parameters near to reference case (TH Kenna, 2000), production $qR_{15}$ is determined by following empirical equation:

$$qR_{15} = 2.125 \cdot 10^8 \left(\frac{U_{\max}}{145}\right)^{0.5} Wm^{-1}, \quad (3)$$

Here $U_{max}$ is maximum tangent wind velocity at given instance of time in knots.

### 2.2 The Second Approximation

Analysis of ETM in the second approximation (SAP) covers general case of TH of non-circular geometry (Fig. 3). By the goal of utilization of TH parameters reflected in regular forecast advisories TH radius at tangent winds 34 knots (17.5 m $s^{-1}$) is accepted as TH outer boundary. Integral heat flow (sensitive and latent) removed from left behind sea strip may be written in following form:

$$A_{34} q = C_i Q W_{34} \left(U_{bb} - U_{dr}\right) \quad (4)$$

Here the nomenclature corresponds to Fig. 3; q is averaged inside $A_{34}$ integral heat flux to TH; Q is averaged inside $A_{34}$ HHP; $U_{bb}$ is translation speed of TH back boundary center; $W_{34}$ ($U_{bb}$-$U_{dr}$), to a certain approximation, determines increment of cooled sea surface.

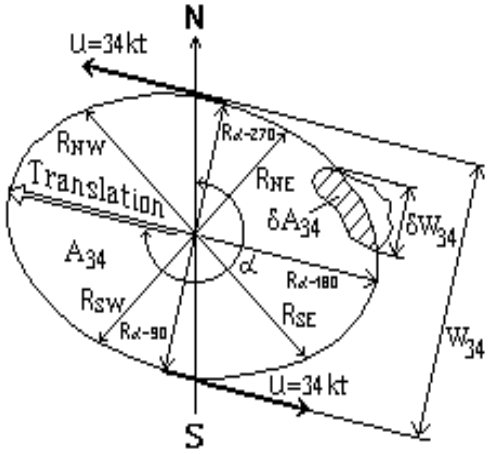


Fig. 3. Scheme of non-circular TH translation: $A_{34}$ is area inside tangent velocity 34 knots (17.5 m $s^{-1}$); $R_{NE}$, $R_{SE}$, $R_{SW}$ and $R_{NW}$ are TH radii at tangent velocity 34 knots in Northeast, Southeast, Southwest and Northwest quadrants, respectively; $\alpha$ is TH translation azimuth; $W_{34}$ is TH transverse width at tangent velocity 34 knot; $\delta A_{34}$ is an area of land surface covered by $A_{34}$; $\delta W_{34}$ is projection onto $W_{34}$ of the part of the back boundary of $A_{34}$ covered by land surface.

Slightly refined value of heat involvement factor also is introduced through SAP based at reanalysis of the field data on TH Opal:

$$C_i \approx \text{Const} = 1/19 \quad (5)$$

Smooth (linear with the angle) distribution of intermediate TH radius is assumed through

calculation of $R_{\alpha\text{-}90}$, $R_{\alpha\text{-}180}$ and $R_{\alpha\text{-}270}$ serving further for determination of TH transverse width and back boundary center coordinates. The area $A_{34}$ is determined as sum of the quadrants using aforementioned 4 values of TH radius. Further, with regard to insignificance of sea surface drift, corresponding to value $C_l \approx 1/19$ condition of establishment of equilibrium translation is written:

$$N_{al} = \frac{\pi W_{34} U_{bb} Q}{2 A_{34} q} = \frac{U_{bb} Q}{q R_{ef}} \approx 30 \qquad (6)$$

Here $R_{ef}$ is effective radius of TH:

$$R_{ef} = 2A_{34} / \pi W_{34} \qquad (7)$$

In such a manner, in the framework of SAP, characteristic linear size of non-circular TH turns to be a function of the square and transverse width of area inside tangent velocity 34 knot.

Further it is necessary to evaluate influence of land surface covering. According to equations (6-7) land surface influences heat balance through reduction of sea surface inside $A_{34}$ and TH active back boundary. Besides, as the first type of influence works through any location of land surface inside $A_{34}$, reduction of back boundary may take place only if it immediately is crossed by land surface.

Reasoning from these deductions accounting of influence of land surface is carried out using correction factors accounting the shares of $\delta A_{34}$ and $\delta W_{34}$ through determination of alignment number. Besides, such a simple approach is applicable only if covered by TH land surface makes comparatively small part of $A_{34}$. In the case of significant share of land surface more detailed additional analysis is necessary.

Finally, it should be noted also that assumption about decisive role of ocean upper layer heat potential naturally restricts applicability of ETM in the case of small TH radius when contribution of initial energy content of environmental air also may become valuable.

### 2.3 Three-zone model of integral heat transfer

Evaluation of average integral heat flux from sea surface to TH turns as the most complicated problem through analysis of individual cases in the framework of ETM. Available results of analysis and field data (Bortkovskiy 1983, Grigorkina 1986, Jacob et al. 2000, D'Asaro 2003, Shekriladze 2004b) on integral heat fluxes have rather wide dispersion (from 0.25 kW $m^{-2}$ to around 4 kW $m^{-2}$). In the context of ETM it represents exceptional importance the records (Shay et al. 2000) of immediate measurement of sensitive and latent heat fluxes made during extremely rapid intensification (to say, during equilibrium translation) of TH Opal in 1995.

Averaging of heat flux within the area inside $A_{34}$ attaches to this parameter certain peculiarities. As area covered by tangent winds in the range 17-25 m $s^{-1}$ makes around 80% of $A_{34}$, this parameter to greater extent depends from heat flux at outer boundary. Besides, within the assumptions made, the last is independent from the most intense tangent winds. At the same time the zone with intense tangent winds also contributes in formation of average heat flux compensating in certain degree the zone's smallness by high values of local fluxes. In this connection adequate evaluation of average heat flux needs accounting of real tangent wind velocity distribution inside $A_{34}$.

In general integral heat flux from ocean upper layer to TH is function of temperature, humidity and velocity fields. Besides, in contrast to single-phase turbulent flow, here decisive role is played by intensity of seawater spraying by tangent winds. As it follows from corresponding analysis general solution of the problem needs further analytical and experimental studies. Below approximate three-zone model is developed focused to equilibrium translation mode.

As it is known (Bortkovskiy 1983, Grigorkina 1986, Shay et al. 2000) dynamical impact of TH on an ocean includes intensive vertical mixing of seawater. Besides, resulted by vertical mixing downward heat flow exceeds sought upward integral heat flow at an order of magnitude (Shay et al. 2000). In this connection vertical mixing becomes decisive factor through transformation of initial SST field. Besides, as it is shown by Goni and Trinanes (2003), this process mainly is restricted by initial HHP. Consequently, these two factors: intensity of vertical mixing and initial HHP level are main factors determining real SST field under TH.

At the same time constancy of involvement factor causes another important peculiarity of heat transfer specifically during equilibrium translation. In general, removal by TH of constant share of HHP needs more time at high

HHP and vice-versa (other things being the same). In this connection equilibrium translation is comparatively slow at high HHP and comparatively fast at low HHP. Accordingly, the area with high initial HHP undergoes more intensive cooling than the area with low initial HHP.

This circumstance allows assuming that SST field under TH is roughly the same irrespective of initial HHP value if translation corresponds to equilibrium mode (other things, to say, tangent wind distribution, being the same). Correspondingly, to a certain approximation, average integral heat flux during equilibrium translation also turns to be independent from initial HHP. It is evident also that the last conclusion, assuming inter-compensating influences of intensity of vertical mixing and initial HHP field, is valid only for equilibrium translation. In such a case average heat flux becomes single-valued function of tangent wind distribution that essentially simplifies further analysis.

Simultaneously the subject matter reduces to near-equilibrium mode of translation restricting applicability of the approach outside of this mode. However, at this stage such a specializing is quite allowable in respect to our focusing to equilibrium translation.

Further, having in account field data structure of regular forecast advisories, three-zone model of heat transfer is introduced. The first (outer) zone covers the area between tangent winds 34 knot (17.5 m $s^{-1}$) and 50 knot (25.75 m $s^{-1}$). The second (intermediate) zone covers the area between tangent winds 50 knot and 64 knot (33 m $s^{-1}$). The third (central) zone covers the area inside tangent wind 64 knot. Within used approach maximum tangent wind influences integral heat transfer only in central zone. Besides, influence of central zone on average integral heat flux is smoothed by comparatively small share of this zone in $A_{34}$ (5 - 15 %).

Further, reasoning from all above and using available field data, following empirical equation is developed for average integral heat flux from sea surface to TH:

$$q = [375(R_1^2-R_2^2)+600(R_2^2-R_3^2)+$$

$$+1600(U_{max}/155)R_3^2]R_1^{-2}\ W\ m^{-2} \qquad (8)$$

Here $R_1$, $R_2$ and $R_3$ are average outer radii in meters of first, second and third zones determined as a quarter of square root from sum of squares of corresponding radii in aforementioned four quadrants; $U_{max}$ is maximum tangent wind velocity inside TH at given position in knots. Characteristic for the first and second zones values 375 W $m^{-2}$ and 600 W $m^{-2}$ are determined through analysis and rounding the data recorded during rapid intensification of TH Opal (Shay et al. 2000). The value 1600 W $m^{-2}$ is determined through equating of arithmetic mean of 8 values of alignment number of super-typhoons Dianmu (2004) and Chaba (2004) at intensity 155 knot to 30.

Finally, it should be noted also that revealed by equation (8) strong dependence of integral heat flux from tangent wind velocity (in comparison with single-phase turbulent heat transfer) looks quite reasonable in the context of decisive role of sea water spraying.

## 3. CORRELATION OF THE FIELD DATA

The main objective of correlation of the field data in the framework of equations (6-8) is verification of predicted by ETM linkage of TH rapid intensification to alignment number (alignment effect).

TH translation speed ($U_{bb}$) is determined through geographical coordinates of TH back boundary center as arithmetic mean of average values for straight translation at two lengths of standard track data prior and subsequent to given position. In certain degree accuracy of this procedure may be assessed using two other alternative procedures of determination of $U_{bb}$ through average values only for one length of standard track data prior or subsequent to given position.

Comparison of aforementioned three alternative values allows to revealing TH translation with significantly variable speed or through curved or zigzagging trajectory when received procedure may turn to be a priori inapplicable. In any case unavailability of local values of translation speed affects accuracy of correlation although in majority of cases situation is mitigated by rather straight and uniform translation of TH just at the stage of rapid intensification.

The problem with initial data precision manifests itself also with HHP. Following from the results of comparative consideration of different HHP maps (NRL hurricane heat potential maps 2004-2005, Goni and Trinanes - hurricane heat potential maps, 2004-2005, Cook - hurricane heat potential maps, 2004-2005), the maps Goni and Trinanes hurricane heat potential

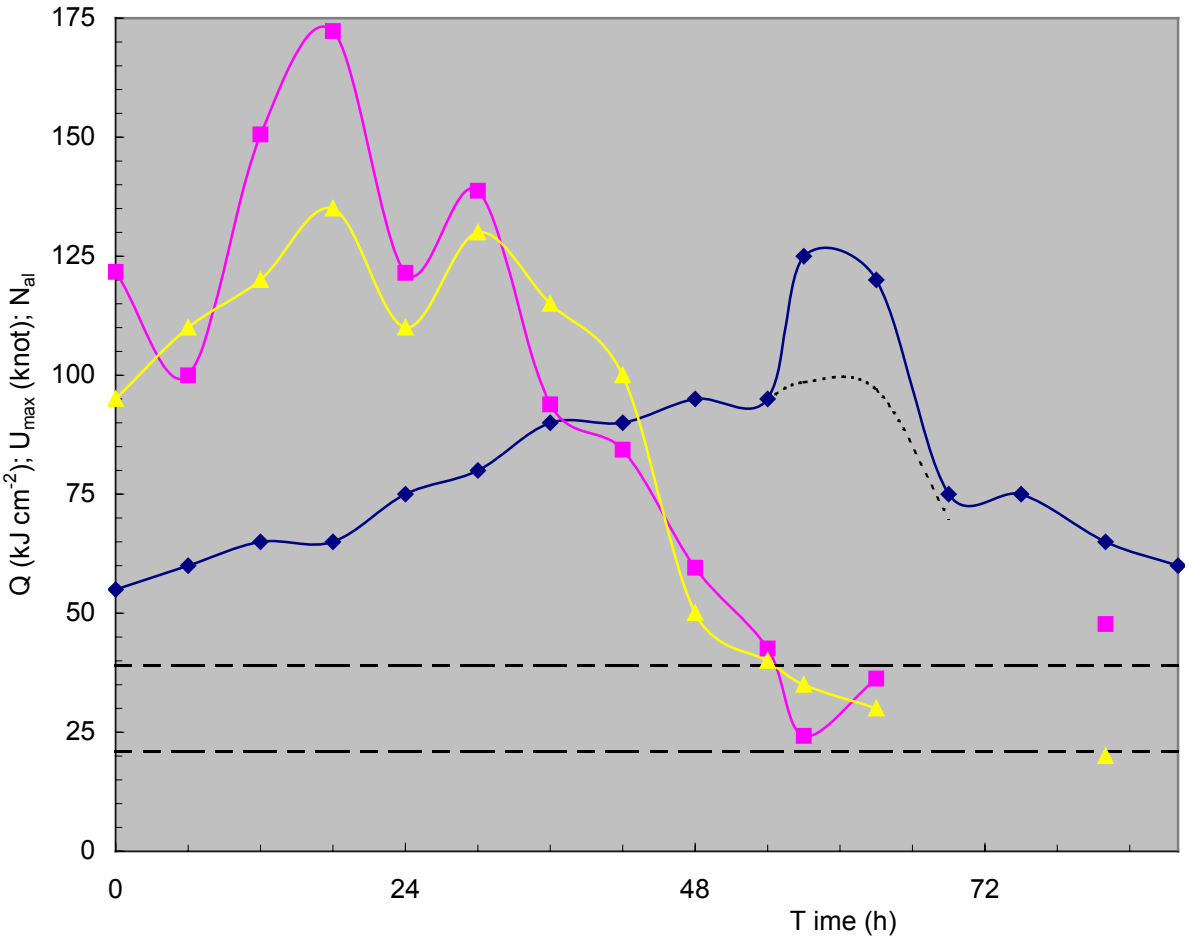


Fig. 4. Correlation of the field data on TH Charley (North West Atlantic, August, 2004) with equations (6-8): triangles - Q (kJ $cm^{-2}$); rhomboids - $U_{max}$ (knot); dotted curve - regular forecast issued 15: 00 (UT) 13.08.2004; squares - $N_{al}$; horizontal lines - the range $N_{al}$=30±30%; blank spaces at 69-75th hours correspond to crossing Florida Peninsula; the point 0 corresponds to 09:00 (UT) 11.08. 2004.

maps (2004-2005) are selected as a basis for consideration.

The stage of rapid intensification is specified by intensification rate no less than 5,0 knot/h and achievement of minimum 4th category of intensity. Following 8 THs are identified as satisfying such a condition among all THs observed in 2004-2005 in all relevant zones of Tropical Ocean: hurricanes Charley, Katrina and Wilma (North West Atlantic), super typhoons Dianmu and Chaba (North West Pacific), cyclones Nancy and Olaf (South Pacific) and Ingrid (South Pacific and South Indian).

Aforementioned correction factors to $A_{34}$ and $W_{34}$ are used through accounting of influence of partial land covering only if corresponding reduction is no more than a third of either of these two parameters. At TH positions, when greater reduction of $A_{34}$ or $W_{34}$ takes place, alignment number is considered as uncertain in developed framework quantity that is reflected in corresponding figures by blank spaces. The results of correlation of some important cases are presented in Figures 4-8.

The first among considered cases is TH Charley, which relates to the number of the most disastrous cases of unexpected rapid intensification. Springing at east boundary of Caribbean Sea Charley passes Northwest approaching west end of Cuba. As it follows from Fig. 4, despite very high values of HHP (100-130 kJ $cm^{-2}$), Charley develops quite moderately at this stage that should be linked to significant excursion of its real translation from equilibrium mode ($N_{al}$≈80-150).

Crossing Cuba and turning north to Florida Peninsula Charley is found in the zone with significantly lower HHP (30-40 kJ $cm^{-2}$).

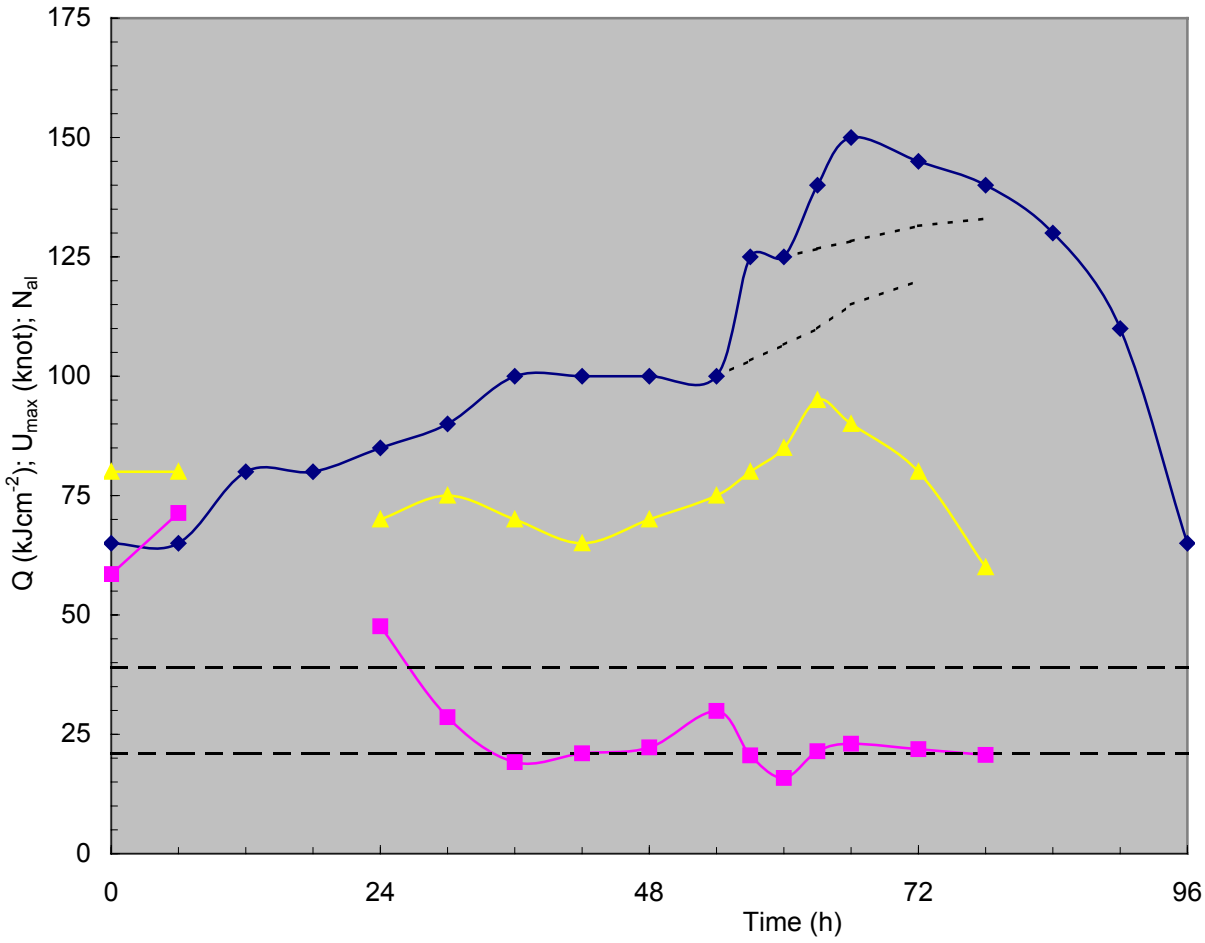


Fig.5. Correlation of the field data on TH Katrina (North West Atlantic, August, 2005) with equations (6-8): triangles - Q (kJ $cm^{-2}$); rhomboids - $U_{max}$ (knot); dotted curves - regular forecasts issued 03:00 (UT) and 09:00 (UT) 28.08. 2005; squares - $N_{al}$; horizontal lines - the range $N_{al}=30\pm30\%$; blank spaces at 12-18th hours correspond to crossing Florida Peninsula, at 84-96th hours - to entering continental part of USA; the point 0 corresponds to 21:00 (UT) 25.08. 2005.

Alignment number significantly reduces (from around 80 to around 25). Charley's translation immediately approaches equilibrium translation mode and Charley strengthens very rapidly (from 95 to 125 knot) during only 3 hours.

Unfortunately, Charley's unexpected intensification took place just prior to landfall to Florida Peninsula. Besides, intensification rate at this stage (10 knot/h) is second high among all selected cases of rapid intensification. Correspondingly, as Charley's rapid intensification is observed against rather sharp reduction of HHP, considered sequence of events clearly demonstrates crucial role of alignment effect in the observed phenomenon. At the same time the effect evidently is overlooked by numerical models serving through preparation of regular forecasts.

Differing sequence of events is observed during development of TH Katrina (Fig. 5). Springing in the zone of Bahamas Islands Katrina crosses Florida Peninsula and Gulf of Mexico making final landfall in the zone of New Orleans. Consequent to establishment of extremely favorable for alignment effect conditions ($N_{al}\approx20$-30; $Q\approx70$-80 kJ $cm^{-2}$) Katrina strengthens in central part of the Gulf from 100 to 125 knot during only 3 hours (intensification rate 8.33) achieving consequent to short-time "respite" intensity 150 knot. Further Katrina weakens alongside with reduction of both of these parameters although it retains extremely dangerous level of intensity up to landfall. (Katrina made landfall as TH of 4th category).

As alignment number holds favorable for TH intensification range during almost all life cycle of

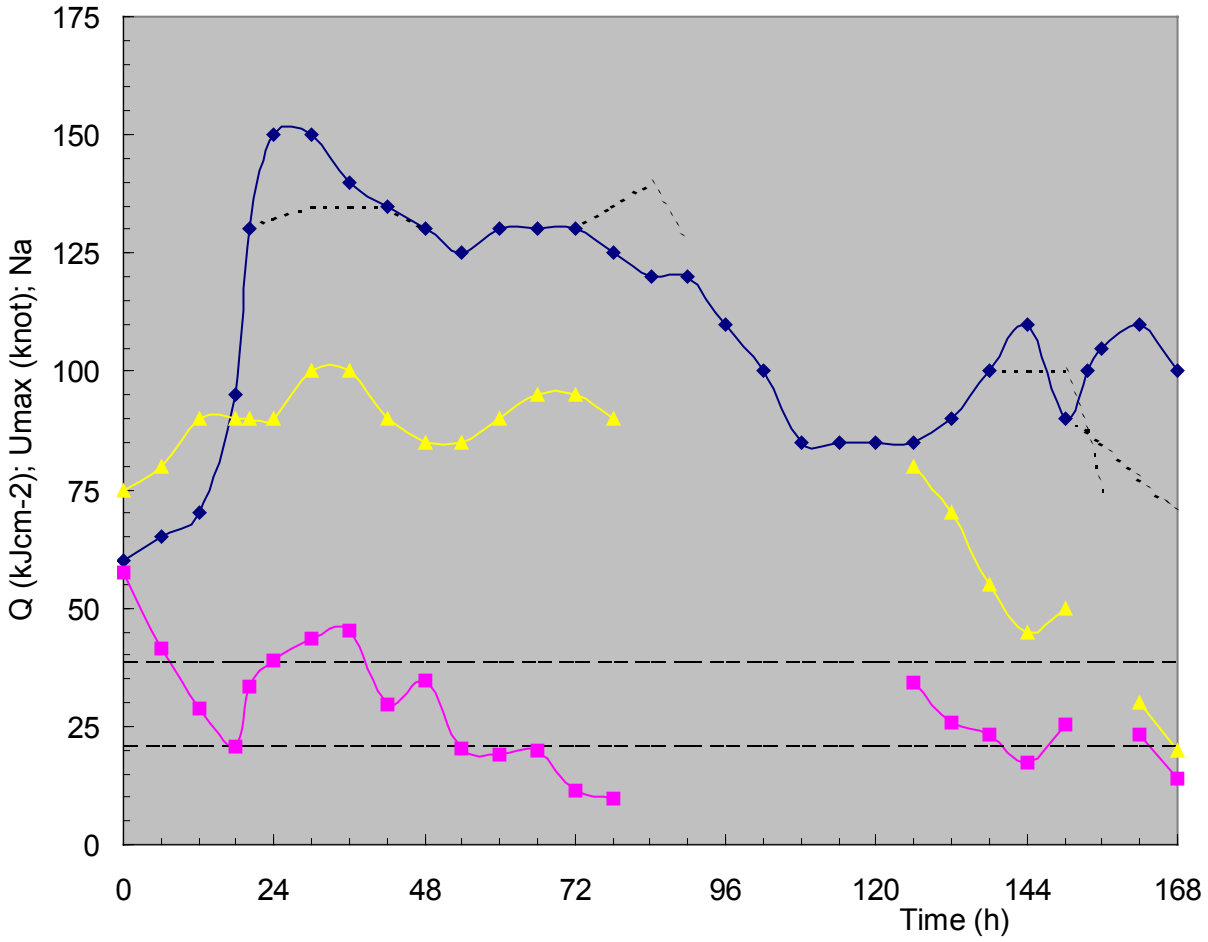


Fig. 6. Correlation of the field data on TH Wilma (North West Atlantic, October, 2005) with equations (6-8): triangles - Q (kJ $cm^{-2}$); rhomboids - $U_{max}$ (knot); dotted curves - regular forecasts issued 05:00 (UT) 19.10.2005, 09:00 (UT) 21.10.2005, 03:00 (UT) and 21:00 (UT) 24.10.2005; squares - $N_{al}$; horizontal lines - $N_{al}$=30±30%; blank spaces at 84-120 hours correspond to covering of Yucatan Peninsula, at 153-156 hours - to crossing Florida Peninsula; the point 0 corresponds to 09:00 (UT) 18.10. 2005.

Katrina, in contrast to Charley, variation of HHP naturally gains leading role in TH development. This circumstance clearly is reflected in Fig. 5 by similarity of TH intensity and HHP curves. Correspondingly, forecasting misses also are comparatively insignificant.

The last is TH Wilma (Fig. 6) among cases of rapid intensification observed in 2004-2005 in North West Atlantic. Springing in central part of Caribbean Sea with high values of HHP (70-95 kJ $cm^{-2}$), Wilma passes northwest, hits Yucatan Peninsula and turns northeast to Florida.

Further Wilma, touching firstly west end of Cuba, crosses Florida Peninsula. Although Wilma starts at rather high alignment numbers ($N_a$≈55) its translation promptly approaches equilibrium mode explosively intensifying from 95 to 130 knot with record-breaking intensification rate 17.5 knot/h during 2 hours. For 4 more hours Wilma achieves 150 knot.

Alternating stages of intensity attenuation and re-intensification, further Wilma remains as rather strong TH of 3rd category through crossing Florida Peninsula.

As it follows from Fig. 6 Wilma's intensity curve adequately correlates with alignment number. At the same time, except underestimation of forthcoming rapid intensification, regular forecasts repeatedly fail in prediction of intensity changes, including overlooking of continuation of Wilma's intensification through landfall to Florida Peninsula and re-intensification through entering North Atlantic.

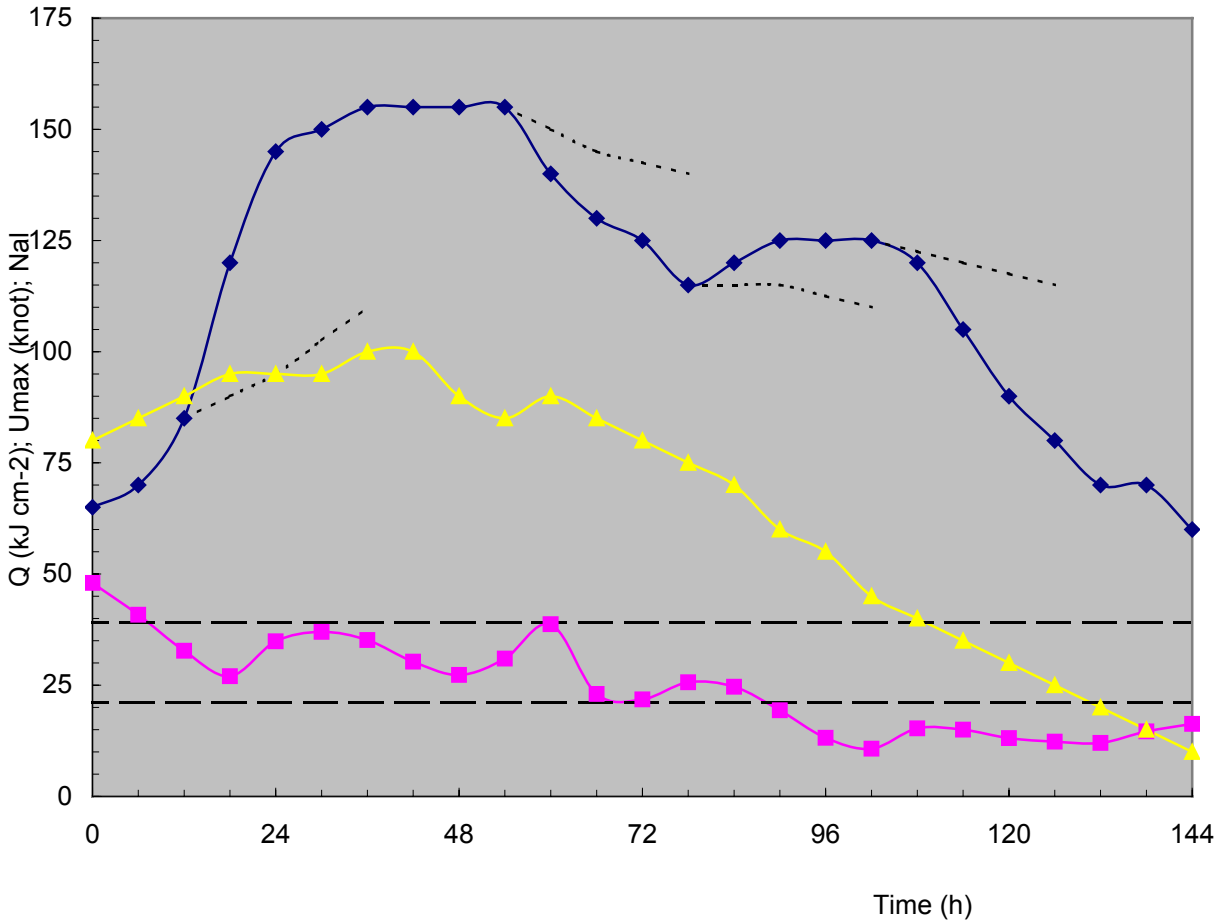


Fig. 7. Correlation of the field data on super typhoon Dianmu (North West Pacific, June, 2004) with equations (6-8): triangles - Q (kJ $cm^{-2}$); rhomboids - $U_{max}$ (knot); dotted curves - regular forecasts issued 06:00 (UT) 16.06.2004, 00:00 (UT) 17.06.2004, 00:00 (UT) 18.06.2004 and 00:00 (UT) 19.06.2004; squares - $N_{al}$; horizontal lines - $N_{al}$=30±30%; the point 0 corresponds to 18:00 (UT) 14.06. 2004.

Combined influence of alignment number and HHP clearly is revealed also through correlation of the filed data on super typhoon Dianmu (Fig. 7) that has developed up to record high for 2004 155-knot intensity in North West Pacific.

As it follows from Fig. 7, consequent to reduction of alignment number to around 30 and corresponding approach to equilibrium translation mode Dianmu rapidly strengthens from 85 to 120 knot during 6 hours with intensification rate equal to 5.83.

Subsequent to Dianmu super typhoon Chaba (Fig. 8) repeats record high for 2004 155-knot intensity in North West Pacific. Starting with rather high values of alignment number in the zone with rather high HHP (100-115 kJ $cm^{-2}$), translation of Chaba promptly approaches equilibrium mode. Simultaneously Chaba rapidly strengthens from 125 to 155 knot during 6 hours with intensification rate 5.0. Besides, correlation between TH intensity and $N_{al}$ is observed during almost all life cycle of Chaba. In this connection Chaba keeps very high intensity even through tangible reduction of HHP.

Crucial role of alignment effect through TH rapid intensification is clearly demonstrated also through correlation of the field data on cyclone Nancy (Fig. 9). Besides, in full contrast to regular forecast, TH rapid intensification with intensification rate 6.25 starts from the very beginning within the range $N_{al}$≈30. During 12 hours intensity of Nancy increases from 45 to 120 knot achieving further maximum level 125 knot. At 24th hour Nancy begins to weaken also in full contrast with regular forecast.

Similar situation is observed also through rapid intensification of cyclone Ingrid in the Gulf of Carpentaria (Fig. 10). Ingrid strengthens from 80 to 120 knot with intensification rate 6.67

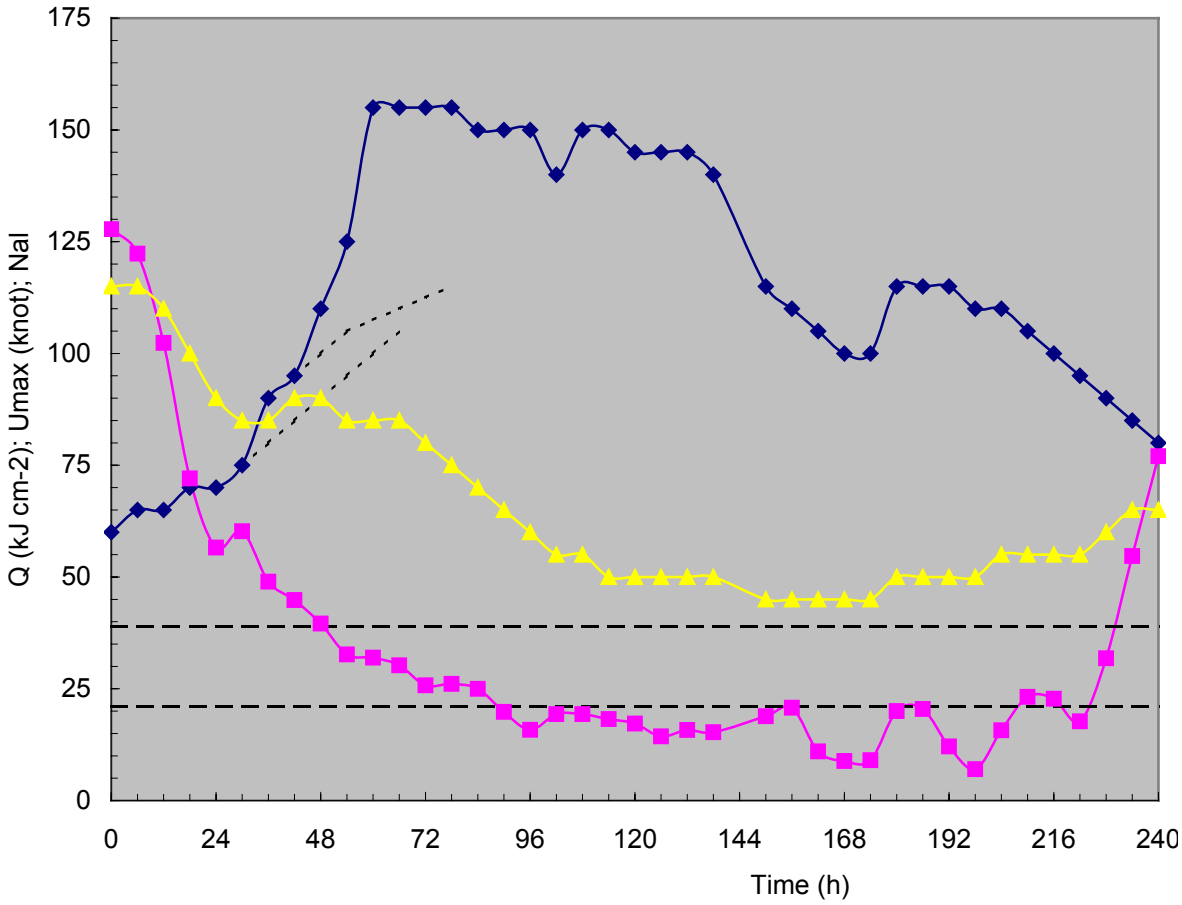


Fig. 8. Correlation of the field data on super typhoon Chaba (North West Pacific, August, 2004) with equations (6-8): triangles - Q (kJ $cm^{-2}$); rhomboids - $U_{max}$ (knot); dotted curves - regular forecasts issued 12:00 (UT) 21.08.2004; 00:00 (UT) 22.08.2004; squares - $N_{al}$; horizontal lines - $N_{al}$=30±30%; the point 0 corresponds to 06:00 (UT) 20.08. 2004.

within the range $N_{al}$=20-30. It presents interesting peculiarity of Ingrid's development existence of 3 phases of intensification during its life cycle. Besides, among all considered cases Ingrid represents exclusive case when the rapidest intensification takes place in the mode of re-intensification.

As a whole, the conclusion on leading role of alignment effect through TH rapid intensification equally is supported by correlation of all selected cases except cyclone Olaf (Fig. 11) that deserves of special consideration.

As it follows from Fig. 11, rapid intensification of Olaf (from 90 to 125 knot during 6 hours with intensification rate 5.83) takes place at rather high values of alignment number ($N_{al}$≈200-90).

According to corresponding analysis, this miscorrelation may be linked to small radius of Olaf. As it was mentioned above, small TH radii restrict applicability of ETM when assumption about decisive role of ocean upper layer heat content may lose its force and contribution of initial energy content of environmental air also may become valuable.

Really, Olaf has the smallest average radius at tangent velocity 50 knot to the end of rapid intensification ($R_2$=56 km) among all cases (the radius $R_2$ is selected here as TH parameter most suitable for evaluation of the role of oceanic heat removal). Among considered cases maximum value of $R_2$ takes place during rapid intensification of super- typhoon Chaba ($R_2$=142 km). Neighbor to Olaf values of this parameter are observed in the cases of cyclone Ingrid ($R_2$=71 km) and TH Charley ($R_2$=84 km). At that leading role of alignment effect clearly manifests itself in both of these cases.

Such a contrast between TH Olaf, on the one hand, and THs Ingrid and Charley, on another, partly may be caused also by high

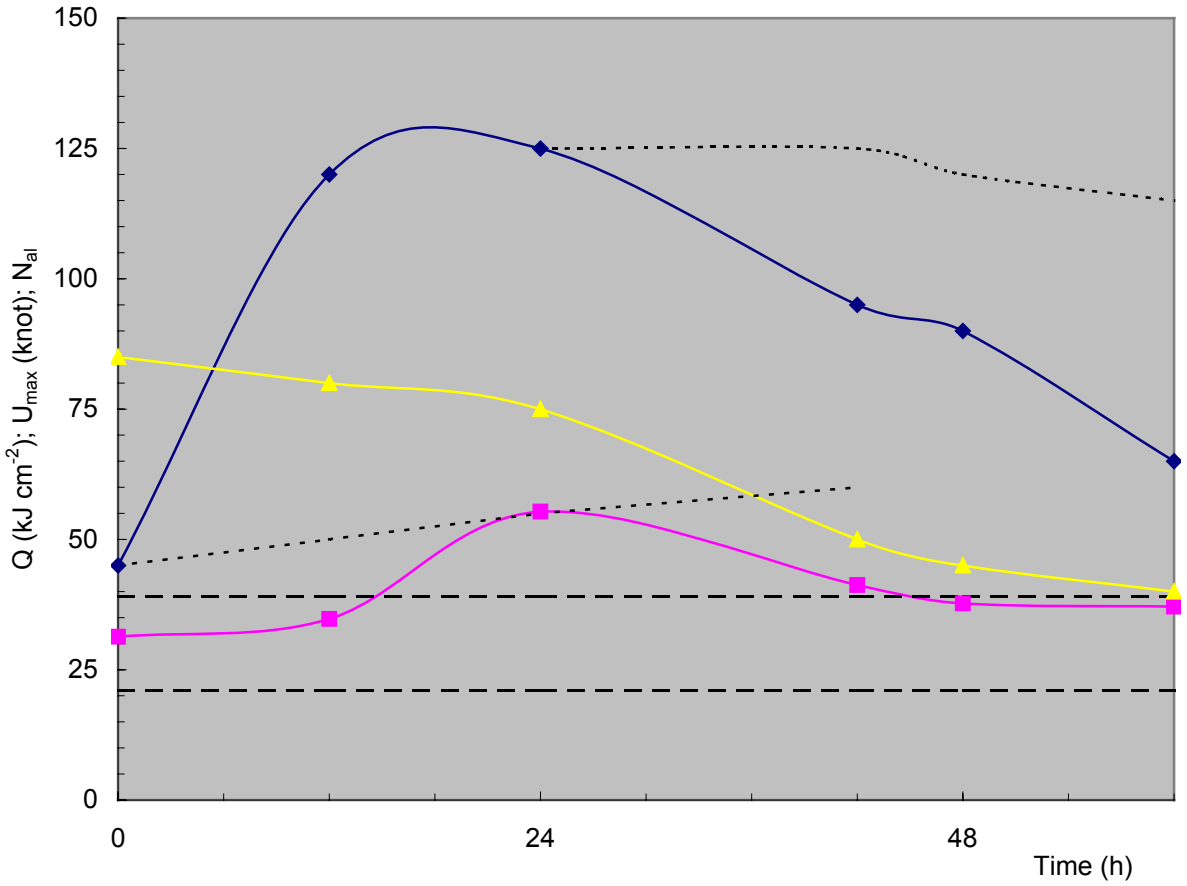


Fig.9. Correlation of the field data on cyclone Nancy (South Pacific, February, 2005) with equations (6-8): triangles - Q (kJ $cm^{-2}$); rhomboids - $U_{max}$ (knot); dotted curves - regular forecasts issued 18:00 (UT) 13.02. 2005 and 18:00 (UT) 14.02. 2005; squares - $N_{al}$; horizontal lines - the range $N_{al}$=30±30%; the point 0 corresponds to 18:00 (UT) 13.02. 2005.

humidity of Olaf's inflow formed above extent open sea area of South Pacific with very high HHP (120-140 kJ $cm^{-2}$).

In contrast to it contribution was significant of comparatively dry continental air through inflow formation in the cases of rapid intensification of TH Ingrid in the region of the Gulf of Carpentaria and TH Charley in the region of Florida Strait.

However, relevance range of ETM requires further detailed study.

## 4. CONCLUDING REMARKS

Predicted by ETM alignment effect manifests itself in overwhelming majority of cases of TH rapid intensification observed in 2004-2005 in all relevant zones of Tropical Ocean (in 7 cases from 8 cases in total). Combined influence of alignment effect and HHP on TH intensity also is established although in some cases alignment effect takes place even against significant reduction of HHP.

Preliminary rough evaluation also is made of limitations of ETM linked to initial energy content of air inflow in the range of small radii of TH.

Comprehensive essence is revealed of Non-dimensional alignment number (incorporating main integral parameters of the system TH-ocean) as a measure of conformity of dynamical and thermal fields.

Unified algorithm is developed describing wide field data without use of any fitting coefficient variable from one TH to another.

The potential of qualitative physical models once again is demonstrated to discover basic features of any subject matter, on this occasion, by the example of exclusively complex and powerful multi-scale natural phenomenon.

Further development of MET and incorporation of alignment effect into numerical models are necessary next steps toward

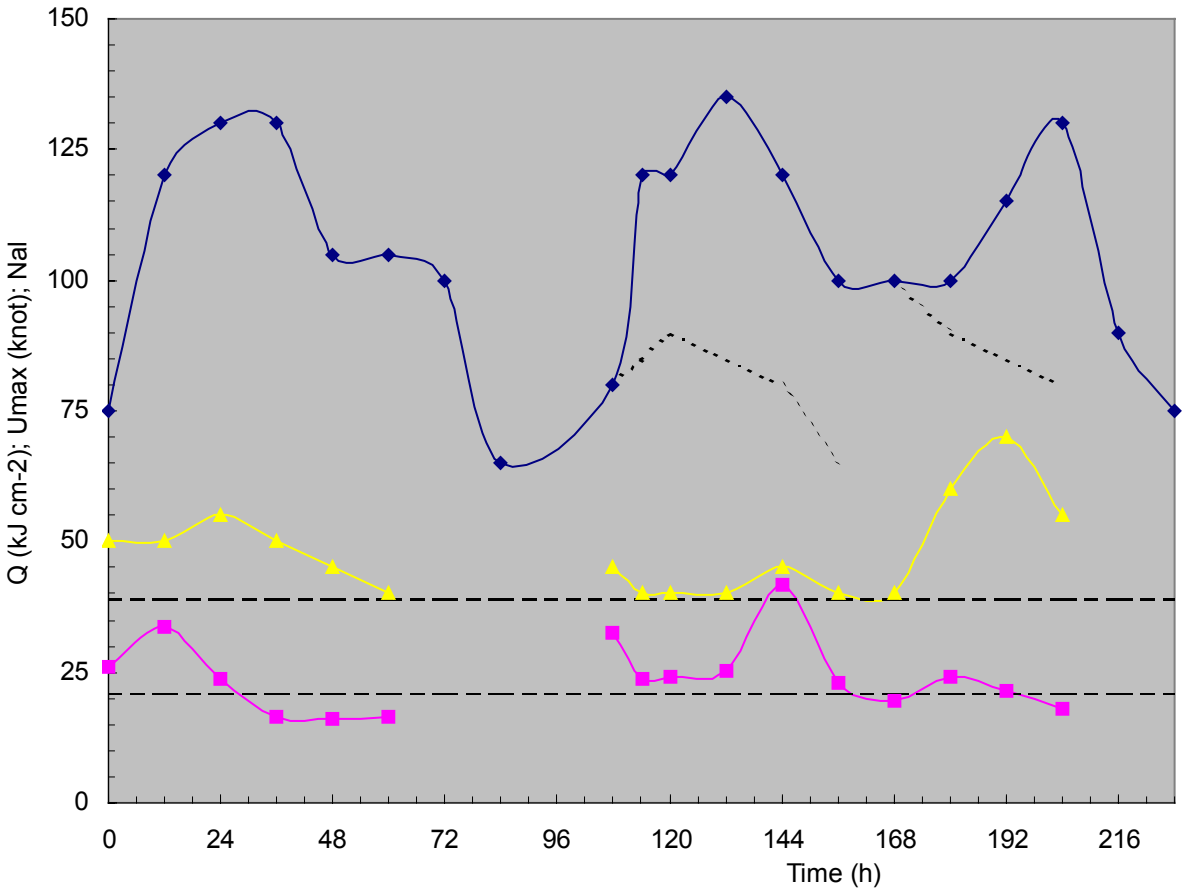


Fig. 10. Correlation of the field data on cyclone Ingrid (South Pacific and South Indian, March, 2005) with equations (6-8): triangles - Q (kJ $cm^{-2}$); rhomboids - $U_{max}$ (knot); dotted curves - regular forecasts issued 06:00 (UT) 11.03. 2005 and 18:00 (UT) 13.03. 2005; squares - $N_{al}$; horizontal lines - the range $N_{al}$=30±30%; blank spaces at 72-84th hours correspond to crossing Cape Peninsula, at 216-218th hours - to covering of north coast of Australia; the point 0 corresponds to 18:00 (UT) 06.03.2005.

qualitative improvement of TH intensity forecasting. At the same time developed here algorithm already allows evaluation of current regular forecasts in real-time mode.

Investigation of the effect may contribute also in clarification of vital problem of potential influence of global warming on regional features of development of tropical hurricanes.

As correlation is decisive of TH equilibrium translation with prevailing regional winds, in some cases elevation of HHP may lead even to hindering of TH development (by mistuning of TH translation and heat removal). Otherwise, reduction of HHP may cause opposite effect.

In this context, the most unwanted scenarios may be realized in the regions where long-term elevation of HHP is accompanied by favorable for alignment effect transformation of correlation between equilibrium mode of TH translation and prevailing regional winds.

**REFERENCES**


1. Bortkovskiy, R. S., 1983: *Atmosphere-Ocean Heat and Moisture Exchange at Storm Conditions (in Russian).* Gidrometeoizdat, 160 pp.
2. Cook, T., 2005: HHP maps (http://storm.rsmas.miami.edu/~nick/heat/).
3. Corbosiero, K. L., Molinary, J., and M. L. Black, 2005: The Structure and Evolution of Hurricane Elena (1985). Part I. *Monthly Weather Review* **133**, 2905–2921.
4. D'Asaro, E. A., 2003: The Ocean Boundary Layer below Hurricane Dennis. Journal of Phys. Oceanogr. **33**, 561–579.
5. Emanuel, K. A., 1999: Thermodynamic control of hurricane intensity. *Nature* **401**, 665 – 669.
6. Emanuel, K. A., 2005, Increasing destructiveness of tropical cyclones over the

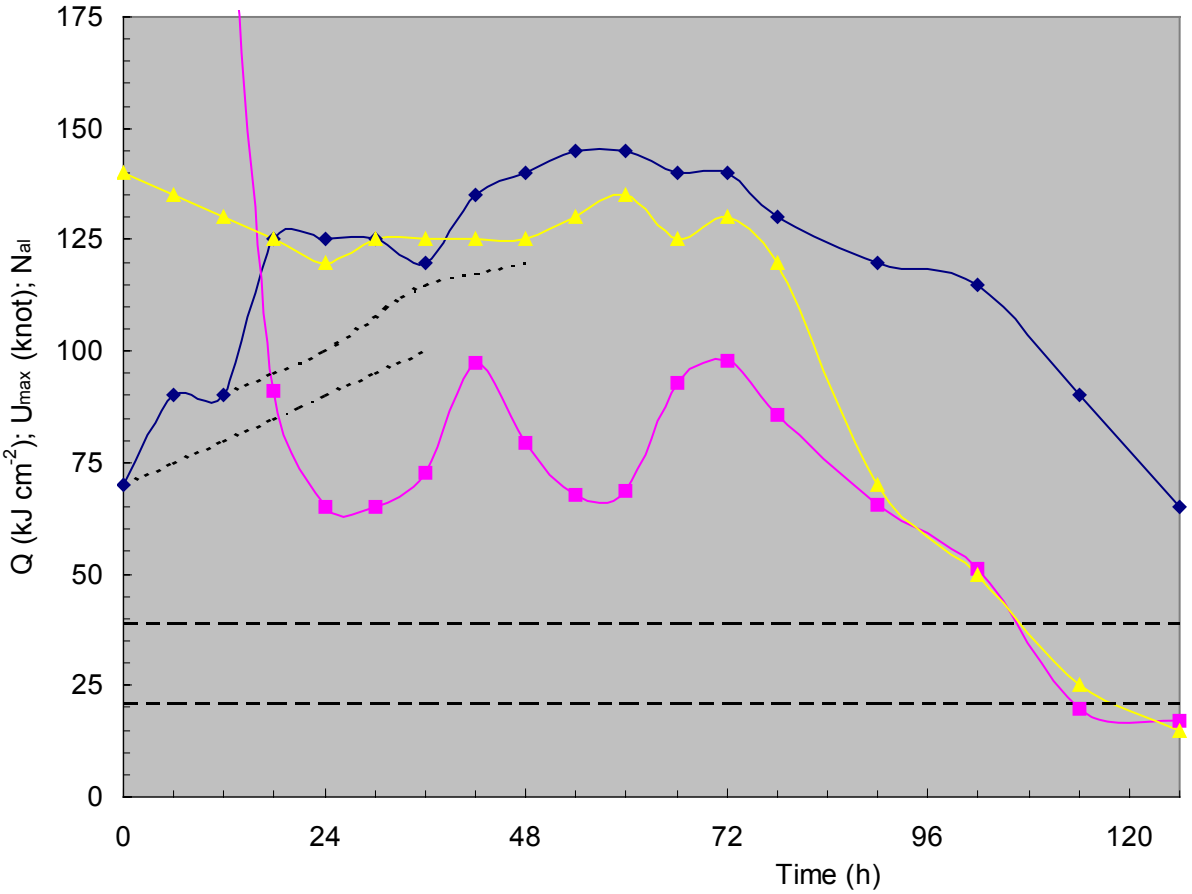


Fig. 11. Correlation of the field data on cyclone Olaf (South Pacific, February, 2005) with equations (6-8): triangles - Q (kJ $cm^{-2}$); rhomboids - $U_{max}$ (knot); dotted curves - regular forecasts issued 00:00 (UT) and 12:00 (UT) 14.02.2005; squares - $N_{al}$; horizontal lines - $N_{al}$=30±30%; the point 0 corresponds to 00:00 (UT) 14.02. 2005.


past 30 years. *Nature* **436**, 686-688.

7. Goldenberg, S. B., Landsea, C. W., Mestas-Nunez, A. M., and W. M. Gray, 2001: The recent increase in Atlantic hurricane activity: causes and implications. *Science* **293**, 474-479.
8. Goni, G. J., and J. Trinanes, 2003: Ocean Thermal Structure Monitoring Could Aid in the Intensity Forecast of Tropical Cyclones. *EOS Transactions*, **84**, 573-580.
9. G. J. Goni, J. Trinanes, HHP maps, 2005: (http://www.aoml.noaa.gov/phod/cyclone/data)
10. Grigorkina, R. G., and B. P. Fux, 1986: *Influence of typhoons on ocean (in Russian).* Gidrometeoizdat, 242 pp.
11. Jacob, S. D., Shay, L. K., Mariano, A. J., and P. G. Black, 2000: The 3-D Oceanic Mixed Layer Response to Hurricane Gilbert. *Journal of Phys. Oceanogr.* **30**, 1407-1429.
12. Kerr, R. A., 2005: Katrina a Harbinger of Still More Powerful Hurricanes? *Science* **308**, 1807-1807.
13. Krishnamurti, T. N., Pattnaik, S., Stefanova, L., Vijaya Kumar, T. S. V., Mackey, B. P., O'Shay, A. J., and R. J. Pasch, 2005: The Hurricane Intensity Issue. *Monthly Weather Review* **133**, 1886–1912.
14. Leipper, D. F. and D. Volgenau, 1972: Hurricane heat potential of the Gulf of Mexico. *J. Phys. Oceanogr.* **2**, 218-224.
15. Lin, I. I., Wu, C. C., Emanuel, K. A., Lee, I. H, Wu, C. R., and I. F. Pun, 2005: The Interaction of Supertyphoon Maemi (2003) with a Warm Ocean Eddy. *Monthly Weather Review* **133**, 2635–2649.
16. McGraw-Hill Encyclopedia of Ocean and Atmospheric Sciences, 1980, McGraw-Hill Book Company, 940pp.
17. Möller, J. D., and L. J. Shapiro, 2005: Influences of Asymmetric Heating on Hurricane Evolution in the MM5. Influences of Asymmetric Heating on Hurricane Evolution in

the MM5. *J. Atmos. Sci.* **62**, 3974-3992.
18. NRL HHP maps, 2005: (http://www7320.nrissc.navy.mil/hhc/).
19. Palmen, E. and Newton, C. W., 1969: Atmospheric circulation systems. Academic Press, 603 pp.
20. Persing, J., and M. T. Montgomery, 2005: Is Environmental CAPE Important in the Determination of Maximum Possible Hurricane Intensity? *J. Atmos. Sci.* **62**, 542–550.
21. Shapiro, L. J., and J. D. Moller, 2005: Influence of Atmospheric Asymmetries on the Intensification of GFDL Model Forecast Hurricanes. *Monthly Weather Review* **133**, 2860–2875.
22. Shay, L. K., Goni, G. J., and P. G. Black, 2000: Effects of a Warm Oceanic Feature on Hurricane Opal. *Monthly Weather Review* **128**, 1366–1383.
23. Shekriladze, I., 2004a: Thermo-Hydrodynamical Alignment Effect – Conditions of Realization. *Bull. Georgian Acad. Sc*. **169**, 298-302.
24. Shekriladze, I., 2004b: Two-Zone Model of Heat Transfer from an Ocean to Tropical Hurricane. *Bull. Georgian Acad. Sc*. **169**, 503-507.
25. Trenberth. K., 2005: Uncertainty in Hurricanes and Global Warming, *Science* **308**, 1753-1754.
26. UNISYS Weather: (http://weather.unisys.com/hurricane/archive/)
27. Webber, H. C., 2005a: Probabilistic Prediction of Tropical Cyclones. Part I: Position. *Monthly Weather Review* **133**, 1840–1852.
28. Webber, H. C., 2005b: Prediction of Tropical Cyclones. Part II: Intensity. *Monthly Weather Review* **133**, 1853–1864.
29. Wu, L., and S. A. Braun 2004: Effects of Environmentally Induced Asymmetries on Hurricane Intensity: A Numerical Study. *J. Atmos. Sci.* **61**, 3065–3081.
30. Wu, L., Wang, B.S., and A. Braun, 2005: Impacts of Air–Sea Interaction on Tropical Cyclone Track and Intensity. *Monthly Weather Review* **133**, 3299–3314.
31. Zhu, H., Ulrich, W., and R.K. Smith, 2004: Ocean Effects on Tropical Hurricane Intensification and Inner-Core Asymmetries. *Atmos. Sci.* **61**, 1245-1258.

**APPENDIX**

## PROCEDURE AND TABLES OF CORRELATION OF THE FIELD DATA ON THE CASES OF TH RAPID INTENSIFICATION (2004-2005)

The appendix to the Paper **"EQUILIBRIUM TRANSLATION MODEL – A KEY TO PREDICTION OF TROPICAL HURRICANE INTENSITY"** contains detailed description of the algorithm of correlation of the field data on tropical hurricane (TH) rapid intensification in the framework of the second approximation (SAP) of equilibrium translation model (ETM), results of correlation of all 8 cases of rapid intensification observed in 2004-2005 in all relevant zones of Tropical Ocean (including tables of correlation). Numbering of equations and figures continues corresponding numbering of the Paper. Made in the appendix references correspond to the chapter of the Paper "REFERENCES".

### 1. TH geometrics

Presented in Fig.3 idealized non-circular contour is based at 4 values of TH radius at tangent velocity 34 knot in Northeast, Southeast, Southwest and Northwest quadrants ($R_{NE}$, $R_{SE}$, $R_{SW}$, $R_{NW}$) specified in regular advisories ($45^0$, $135^0$, $225^0$ and $315^0$ from North, respectively) according to UNISYS Weather.

At first stage four radii $R_\alpha$, $R_{\alpha\text{-}90}$, $R_{\alpha\text{-}180}$ and $R_{\alpha\text{-}270}$ are determined through simple smooth trigonometric interpolation of aforementioned initial data:

$$R_\alpha = R_{SW} - \frac{R_{SW} - R_{NW}}{90}(\alpha - 315) \tag{9}$$

$$R_{\alpha-90} = R_{SE} - \frac{R_{SE} - R_{SW}}{90}(\alpha - 90 - 135) \tag{10}$$

$$R_{\alpha-180} = R_{NE} - \frac{R_{NE} - R_{SE}}{90}(\alpha - 180 - 45) \tag{11}$$

$$R_{\alpha-270} = R_{NW} - \frac{R_{NW} - R_{NE}}{90}(\alpha - 270 + 45) \tag{12}$$

Further TH transverse size ($W_{34}$), average radii at tangent wind with speeds 34 knot, 50 knot and 64 knot ($R_1$, $R_2$ and $R_3$, respectively), an area inside tangent velocity 34 knot ($A_{34}$), coordinates (latitude - $Lt_{bb}$, longitude - $Ln_{bb}$) and translation speed ($U_{bb}$) of TH back boundary center are determined:

$$W_{34} = R_{90} + R_{270} \tag{13}$$

$$R_1 = 0.25\left(R_{NE,34}^2 + R_{SE,34}^2 + R_{SW,34}^2 + R_{NW,34}^2\right)^{0.5} \tag{14}$$

$$R_2 = 0.25\left(R_{NE,50}^2 + R_{SE,50}^2 + R_{SW,50}^2 + R_{NW,50}^2\right)^{0.5} \quad (15)$$

$$R_3 = 0.25\left(R_{NE,64}^2 + R_{SE,64}^2 + R_{SW,64}^2 + R_{NW,64}^2\right)^{0.5} \quad (16)$$

$$A_{34} = (\pi/4)\left(R_{NE,34}^2 + R_{SE,34}^2 + R_{SW,34}^2 + R_{NW,34}^2\right) \quad (17)$$

$$Lt_{bb} = Lt_c \pm \left(R_{\alpha-180}/\left(1.11\cdot 10^5\right)\right)Cos\alpha \quad (18)$$

$$Ln_{bb} = Ln_c \pm \left(R_{\alpha-180}/\left(1.11\cdot 10^5 \cdot CosLt_{bb}\right)\right)Sin\alpha \quad (19)$$

Here $Lt_c$ and $Ln_c$ are corresponding coordinates of TH center specified in corresponding regular advisory; the length of a degree of latitude is accepted as constant and equal to $1.11\cdot 10^5$m; the length of a degree of longitude is accepted as equal to $CosLt_{bb}\cdot 1.11\cdot 10^5$m;

**2. TH back boundary translation**

As the field data specified in regular forecast advisories do not allow determining of local translation speed, $U_{bb}$ at current position is determined through geographical coordinates of TH back boundary center as arithmetic mean of average values for straight translation at two lengths of standard track data prior and subsequent to current position:

$$U_{bb} = \frac{U_{bb-1} + U_{bb+1}}{2} \quad (20)$$

$$U_{bb-1} = \frac{\left(\left(\left(Lt_{bb} - Lt_{bb-1}\right)\cdot 1.11\cdot 10^5\right)^2 + \left(\left(Ln_{bb} - Ln_{bb-1}\right)\cdot 1.11\cdot 10^5 CosLt_{bb}\right)^2\right)^{0.5}}{\tau - \tau_{-1}} \quad (21)$$

$$U_{bb+1} = \frac{\left(\left(\left(Lt_{bb+1} - Lt_{bb}\right)\cdot 1.11\cdot 10^5\right)^2 + \left(\left(Ln_{bb+1} - Ln_{bb}\right)\cdot 1.11\cdot 10^5 CosLt_{bb}\right)^2\right)^{0.5}}{\tau_{+1} - \tau} \quad (22)$$

Here subscripts -1 and +1 correspond to TH positions and lengths of standard track data prior and consequent to current position according regular advisories, respectively.

Unavailability of local values of translation speed affects accuracy of correlation in any case although in majority of cases situation is mitigated by rather straight and uniform translation of TH just at the stage of rapid intensification.

In certain degree accuracy of determination through equation (20) may be assessed using alternative procedures of determination of $U_{bb}$ through average values only for one length of standard track data prior or subsequent to given position (through equation (21) or equation (22)). Comparison of aforementioned three values allows to revealing TH translation with significantly variable speed or through curved or zigzagging trajectory.

### 3. Determination of average HHP

The problem with initial data precision manifests itself also with HHP. Among different HHP maps (NRL maps, Goni and Trinanes maps, Cook maps) only NRL maps and the maps of Goni and Trinanes cover all relevant zones of Tropical Ocean. Besides, NRL maps present the most important range of HHP (40-90 kJcm$^{-2}$) by hardly distinguishable colors. In this connection the maps of Goni and Trinanes, characterized by comparatively high color resolvability, are adopted as a basis for our consideration.

HHP is determined as average weighted value for sea surface inside $A_{34}$ for the time point just prior to entering of TH front in given area. Conversion of the color into figures imports human factor affecting accuracy of determination. As TH translation is determined through regular advisories by lag 6 hours, the lag 24 hours between the HHP maps also causes some additional error.

### 4. Integral heat flux

Average inside $A_{34}$ integral heat flux is determined based at three-zone model of heat transfer introduced in the paper. The first zone covers the area between tangent winds 34 knot (17.5 ms$^{-1}$) and 50 knot (25.75 ms$^{-1}$). The second zone covers the area between tangent winds 50 knot and 64 knot (33 ms$^{-1}$). The third zone covers the area inside tangent wind 64 knot. Average integral heat flux is determined through empirical equation (8) of the Paper.

### 5. Correction factors on partial land covering

Accounting of influence of land surface covered by TH is carried out using following correction factors to $W_{34}$ and $A_{34}$ through determination of effective radius according equation (7) and alignment number according equation (6):

$$C_W = 1 - \frac{\delta W_{34}}{W_{34}} \tag{23}$$

$$C_A = 1 - \frac{\delta A_{34}}{A_{34}} \tag{24}$$

### 6. Accuracy of correlation of the field data

Accuracy of correlation of the field data in the framework of equations (6-8) is determined by the procedures of determination of HHP using HHP maps and calculation of $U_{bb}$ and $qR_{ef}$. Errors in determination of these parameters may vary in rather wide range depending from values of parameters themselves. For instance, HHP and $U_{bb}$ determination errors are high at these low absolute values (around ±30% and even more).

An error connected with neglecting of a sea surface drift is rather low in majority of cases (no more than ±5%). Accuracy of equation (8) may be evaluated as ±20%. Some specific errors are connected with accepted way of determination of $U_{bb}$. Firstly, it is intersection by alignment number curve of the zone of alignment effect. As uninterrupted data on $U_{bb}$ are not available, really sharp transition also may take place without realization of any regime inside $N_{al}$=30±30%. So, here we have uncertainty that may be eliminated only using more detailed field data. Secondly, it is connected with mentioned above underestimation of $U_{bb}$ at TH indirect translation.

In such a complicated situation accuracy of correlation in the best way may be characterized by dispersion of the field data. In rather good accordance with ETM dispersion $N_{al}$=30±30% is typical for the stage of rapid intensification of almost all TH involved in correlation. Corresponding level of accuracy of correlation may be accepted for majority of considered cases having in mind that in separate situations correlation may be much less accurate.

## 7. Correlation of the field data

### 7.1. Composition of initial field data involved in correlation

Calculation of alignment number through equations (6-24), in combination with HHP determined using corresponding HHP map, involves following parameters specified in regular advisories:

- Time points and corresponding TH center coordinates at current position and at positions prior and subsequent to current position;
- Maximum tangent wind velocity at current position;
- TH radii at tangent wind velocity 34 knot in Northeast, Southeast, Southwest and Northwest quadrants at current position;
- TH radii at tangent wind velocity 50 knot in Northeast, Southeast, Southwest and Northwest quadrants at current position;
- TH radii at tangent wind velocity 64 knot in Northeast, Southeast, Southwest and Northwest quadrants at current position;
- TH translation azimuth at the length of standard track data prior to current position.

Simultaneously additional parameters are involved such as an area of land surface covered by $A_{34}$ ($\delta A_{34}$) and a projection onto $W_{34}$ of the part of the back boundary of $A_{34}$ covered by land ($\delta W_{34}$) both determined using TH geometrics at current position and geographical map. It should be stressed also that equations (6-24) form unified algorithm designed for description of the field data on different TH using abovementioned initial field data without using of any fitting coefficient variable from one TH to another.

### 7.2. Selection of the cases

The case of rapid intensification is specified by availability of the stage with intensification factor no less than 5.0 knot/h and achievement to the end of the stage of minimum 4th category of intensity. Consideration covers all 8 THs of 4th and 5th category identified as cases of rapid intensification among all tropical hurricanes observed in 2004-2005 in all relevant zones of Tropical Ocean. Selected in such a manner cases are: hurricanes Charley, Katrina and Wilma (North West Atlantic), super typhoons Dianmu and Chaba (North West Pacific), cyclones Nancy (South Pacific), Olaf (South Indian) and Ingrid (South Pacific and South Indian).

### 7.3. Comparison between FAP and SAP

Previous realization of ETM (FAP) is based at assuming of uniform straightforward translation of circular TH of constant size at open sea surface. Heat balance of underplaying sea surface is considered inside TH boundary with tangent wind speed 15 m $s^{-1}$.

In the case of straightforward translation of circular TH of constant size translation speed $U_{bb}$ (determining increment of cooled sea surface) turns to be equal to TH center translation speed ($U_{trc}$). In addition, uniform translation allows determining $U_{trc}$ "as average for straight line covering 2 time intervals of standard track data prior and subsequent to this instance" (Shekriladze 2004a). Accordingly, conditions of alignment effect are reduced to equation (3) of the paper.

Production $qR_{15}$ is determined by empirical equation (4) of the paper based at parameters of TH Kenna. Expansion of the equation linking heat flux only to maximum tangent velocity on all cases refers to assumption in the framework of FAP of similar radial distribution of tangent wind speeds in all THs.

Transition in the SAP to consideration of heat balance inside $R_{34}$ allows using the field data on tangent wind distribution specified in regular forecast advisories. Determination of heat balance based at $U_{bb}$ taking in account TH non-circular geometry allows description of TH curved translation with variable TH's shape. Three-zone model of heat transfer and corresponding empirical equation (7) allow accounting of real radial distribution of tangent wind speed. Introduction of correction factors (23) and (24) also improves description of TH development. At the same time determination of $U_{bb}$ through equation (15) only slightly improves description of curved translation and unavailability of local current values of $U_{bb}$ lowers accuracy of analysis.

As it follows from above, results of FAP and SAP may differ or coincide depending from a number of parameters. As it follows from analysis of such a comparison all considered cases of rapid intensification might be subdivided into three groups.

The first group includes the cases with practically identical correlation of the field data by previous and refined realizations of ETM (TH Katrina, super typhoons Dianmu and Chaba). Rather close coincidence of FAP and SAP may be explained by validity of the approximation underlying FAP of ETM in these cases.

The second group includes the cases with clearly different but rather close curves of correlation of the field data (THs Charley and Wilma, cyclone Nancy). As it follows from corresponding analysis, despite some quantitative differences, FAP adequately describes the process of Charley's development. Besides, it also predicts the stage of rapid intensification although the stage itself is described by SAP evidently better. However, taking in account in addition related sizes of Charley and Kenna (FAPs reference case), FAP of ETM may be considered as an instrument that might be used for prediction of high probability of Charley's rapid intensification through landfall to Florida Peninsula 13th of August 2004. As a whole, more relevant description of TH development by SAP of ETM manifests itself in all cases of this group.

The smallest in number third group includes the cases with significantly differing curves of correlation of the field data by FAP and SAP (cyclones Ingrid and Olaf). Besides, FAP evidently leads to miscorrelation.

Finally, results of comparison may be evaluated as quite valuable. On the one hand, these results demonstrate principal limitations of the FAP (by the way, together with demonstration of sizable area of its applicability as well); on the other hand, qualitative widening becomes evident of covering of different cases of TH rapid intensification by ETM through SAP.

### 7.4. Tables of correlation of the field data in the framework of SAP

Detailed tables of correlation of all considered cases of rapid intensification in the framework of equations (6-24) are presented below. Each row of the table describes certain TH position. The row includes 17 parameters borrowed from regular forecast advisory and value of HHP determined through Goni and Trinanes HHP map. The same row presents the main result of correlation for given TH position: current value of alignment number. Correction factors to $A_{34}$ and $W_{34}$ on partial land covering also are presented. These factors are used only if corresponding reduction is no more than a third of either of these two parameters. Besides, alignment number is considered as uncertain in developed framework quantity at TH positions with greater reduction of. $A_{34}$ or $W_{34}$. Such a situation is reflected by blank spaces in corresponding tables. Dimensions of initial parameters in tables correspond to regular advisories and HHP maps. Each of tables is provided by necessary comments.

# TABLES OF CORRELATION OF TH RAPID INTENSIFICATION CASES OBSERVED IN 2004-2005

Table 1.

Correlation of the field data on TH CHARLEY (West North Atlantics)

| TIME | LAT | LON | $R_{64}$ NE | $R_{64}$ SE | $R_{64}$ SW | $R_{64}$ NW | $R_{50}$ NE | $R_{50}$ SE | $R_{50}$ SW | $R_{50}$ NW | $R_{34}$ NE | $R_{34}$ SE | $R_{34}$ SW | $R_{34}$ NW | $\alpha$ | $C_W$ | $C_A$ | Q | $U_{tn}$ | $N_{al}$ |
|---|---|---|---|---|---|---|---|---|---|---|---|---|---|---|---|---|---|---|---|---|
| (h) | (deg) | (deg) | (knmi) | (knmi) | (knmi) | (knmi) | (knmi) | (knmi) | (knmi) | (knmi) | (knmi) | (knmi) | (knmi) | (knmi) | [grad] | | | (kJ cm$^{-2}$) | (knot) | |
| -6 | 16.0 | 72.8 | | | | | | | | | | | | | | | | | | |
| 0 | 16.9 | 74.7 | | | | | 20 | 0 | 0 | 0 | 100 | 50 | 0 | 75 | 295 | 1.00 | 1.00 | 95 | 55 | 121.7 |
| 6 | 16.5 | 76.1 | | | | | 40 | 0 | 0 | 40 | 100 | 75 | 0 | 75 | 285 | 1.00 | 1.00 | 110 | 60 | 99.9 |
| 12 | 17.0 | 77.5 | 25 | 0 | 0 | 25 | 40 | 0 | 0 | 40 | 100 | 75 | 0 | 75 | 290 | 0.69 | 0.84 | 120 | 65 | 150.6 |
| 18 | 17.8 | 78.7 | 25 | 0 | 0 | 25 | 40 | 0 | 0 | 40 | 100 | 75 | 30 | 75 | 300 | 0.80 | 0.89 | 135 | 65 | 172.3 |
| 24 | 18.6 | 79.9 | 20 | 0 | 0 | 20 | 50 | 20 | 0 | 40 | 100 | 75 | 30 | 75 | 305 | 1.00 | 1.00 | 110 | 75 | 121.5 |
| 30 | 19.7 | 81.2 | 20 | 15 | 10 | 20 | 50 | 30 | 10 | 40 | 100 | 90 | 30 | 75 | 310 | 1.00 | 1.00 | 130 | 80 | 138.7 |
| 36 | 21.2 | 81.9 | 25 | 20 | 10 | 20 | 60 | 50 | 20 | 40 | 110 | 100 | 40 | 90 | 335 | 1.00 | 0.94 | 115 | 90 | 93.9 |
| 42 | 22.2 | 82.4 | 25 | 20 | 10 | 20 | 60 | 50 | 20 | 40 | 110 | 100 | 45 | 90 | 340 | 0.84 | 0.75 | 100 | 90 | 84.3 |
| 48 | 23.9 | 82.9 | 25 | 20 | 10 | 20 | 60 | 50 | 20 | 40 | 110 | 100 | 45 | 90 | 345 | 0.74 | 0.89 | 50 | 95 | 59.6 |
| 54 | 25.2 | 82.8 | 25 | 25 | 15 | 15 | 50 | 50 | 40 | 40 | 90 | 90 | 75 | 75 | 360 | 1.00 | 1.00 | 40 | **95** | 42.6 |
| 57 | 26.0 | 82.4 | 25 | 25 | 15 | 15 | 50 | 50 | 40 | 40 | 90 | 90 | 75 | 75 | 5 | 1.00 | 0.73 | 35 | **125** | 24.2 |
| 63 | 26.9 | 82.2 | 20 | 20 | 0 | 0 | 30 | 40 | 40 | 25 | 40 | 75 | 75 | 50 | 15 | 1.00 | 0.68 | 30 | 120 | 36.3 |
| 69 | 29.1 | 81.1 | 20 | 20 | 20 | 10 | 30 | 40 | 30 | 25 | 40 | 75 | 40 | 40 | 20 | 0.00 | 0.08 | | 75 | |
| 75 | 31.2 | 80.5 | 25 | 50 | 20 | 10 | 50 | 75 | 30 | 25 | 75 | 100 | 40 | 40 | 20 | 0.34 | 0.97 | | 75 | |
| 82 | 33.2 | 79.0 | 25 | 40 | 0 | 0 | 50 | 75 | 0 | 0 | 75 | 100 | 40 | 40 | 25 | 0.74 | 0.76 | 20 | 65 | 47.7 |
| 88 | 36.0 | 77.0 | | | | | | | | | | | | | | | | | | |

The point 0 corresponds to 09:00 UT, August 11, 2004. Rapid intensification (with intensification rate 10 knot/h) is observed at 54-57th hours. Blank spaces at 69-75th hours correspond to crossing Florida Peninsula. $R_2$=84 km at 57th hour.

Table 2.

Correlation of the field data on TH KATRINA (West North Atlantics)

| TIME | LAT | LON | $R_{64}$ NE | $R_{64}$ SE | $R_{64}$ SW | $R_{64}$ NW | $R_{50}$ NE | $R_{50}$ SE | $R_{50}$ SW | $R_{50}$ NW | $R_{34}$ NE | $R_{34}$ SE | $R_{34}$ SW | $R_{34}$ NW | a | $C_W$ | $C_A$ | Q | $U_{tn}$ | $N_{al}$ |
|---|---|---|---|---|---|---|---|---|---|---|---|---|---|---|---|---|---|---|---|---|
| (h) | (deg) | (deg) | (knmi) | (knmi) | (knmi) | (knmi) | (knmi) | (knmi) | (knmi) | (knmi) | (knmi) | (knmi) | (knmi) | (knmi) | [grad] | | | (kJ $cm^{-2}$) | (knot) | |
| -6 | 26.2 | 79.3 | | | | | | | | | | | | | | | | | | |
| 0 | 26.1 | 79.9 | 15 | 15 | 10 | 10 | 25 | 25 | 20 | 20 | 70 | 70 | 50 | 60 | 270 | 1.00 | 0.88 | 80 | 65 | 58.6 |
| 6 | 25.5 | 80.7 | 10 | 10 | 0 | 10 | 20 | 20 | 0 | 20 | 60 | 60 | 30 | 60 | 270 | 1.00 | 0.66 | 80 | 65 | 71.3 |
| 12 | 25.3 | 81.5 | 20 | 20 | 0 | 0 | 60 | 60 | 20 | 0 | 75 | 75 | 40 | 30 | 270 | 0.34 | 0.80 | | 80 | |
| 18 | 25.1 | 82.2 | 20 | 20 | 0 | 0 | 60 | 60 | 20 | 0 | 75 | 75 | 40 | 30 | 270 | 0.45 | 0.97 | | 80 | |
| 24 | 24.8 | 82.9 | 20 | 20 | 15 | 10 | 60 | 60 | 35 | 20 | 75 | 75 | 55 | 35 | 270 | 0.79 | 1.00 | 70 | 85 | 47.6 |
| 30 | 24.6 | 83.6 | 20 | 20 | 15 | 10 | 60 | 60 | 35 | 20 | 75 | 75 | 55 | 35 | 270 | 1.00 | 1.00 | 75 | 90 | 28.6 |
| 36 | 24.4 | 84.4 | 35 | 30 | 30 | 25 | 60 | 60 | 45 | 60 | 130 | 90 | 90 | 130 | 270 | 1.00 | 1.00 | 70 | 100 | 19.2 |
| 42 | 24.5 | 85.0 | 35 | 30 | 30 | 25 | 60 | 60 | 45 | 60 | 130 | 90 | 90 | 130 | 270 | 1.00 | 1.00 | 65 | 100 | 21.0 |
| 48 | 24.6 | 85.6 | 40 | 30 | 30 | 30 | 60 | 60 | 60 | 60 | 140 | 90 | 90 | 130 | 270 | 1.00 | 1.00 | 70 | 100 | 22.3 |
| 54 | 25.0 | 86.2 | 60 | 30 | 30 | 30 | 75 | 60 | 60 | 60 | 140 | 90 | 90 | 130 | 270 | 1.00 | 1.00 | 75 | **100** | 29.9 |
| 57 | 25.1 | 86.8 | 60 | 45 | 45 | 45 | 80 | 80 | 65 | 80 | 140 | 100 | 100 | 140 | 270 | 1.00 | 1.00 | 80 | **125** | 20.6 |
| 60 | 25.4 | 87.4 | 75 | 75 | 50 | 75 | 100 | 100 | 75 | 100 | 160 | 160 | 125 | 140 | 270 | 1.00 | 1.00 | 85 | 125 | 15.9 |
| 63 | 25.7 | 87.7 | 75 | 75 | 50 | 75 | 100 | 100 | 75 | 100 | 160 | 160 | 125 | 140 | 270 | 1.00 | 1.00 | 95 | 140 | 21.5 |
| 66 | 26.0 | 88.1 | 90 | 90 | 50 | 75 | 120 | 120 | 75 | 100 | 180 | 180 | 125 | 140 | 270 | 1.00 | 1.00 | 90 | 150 | 23.0 |
| 72 | 26.9 | 89.0 | 90 | 90 | 50 | 90 | 120 | 120 | 75 | 120 | 200 | 180 | 125 | 180 | 270 | 1.00 | 0.98 | 80 | 145 | 21.9 |
| 78 | 27.6 | 89.4 | 90 | 90 | 50 | 80 | 110 | 100 | 75 | 100 | 200 | 200 | 150 | 180 | 270 | 1.00 | 0.92 | 60 | 140 | 20.7 |
| 84 | 28.8 | 89.6 | 90 | 90 | 50 | 80 | 110 | 100 | 75 | 100 | 200 | 200 | 150 | 180 | 270 | 1.00 | 0.59 | | 130 | |
| 90 | 30.2 | 89.6 | 110 | 110 | 60 | 60 | 140 | 140 | 75 | 75 | 200 | 200 | 150 | 100 | 270 | 1.00 | 0.47 | | 110 | |
| 96 | 31.9 | 89.6 | 50 | 50 | 30 | 30 | 75 | 100 | 75 | 75 | 100 | 180 | 100 | 100 | 270 | 0.38 | 0.19 | | 65 | |
| 102 | 33.5 | 88.5 | | | | | | | | | | | | | | | | | | |

The point 0 corresponds to 21:00 UT, August 25, 2005. Rapid intensification (with intensification rate 8.33 knot/h) is observed at 54-57th hours. Blank spaces at 12-18th hours correspond to crossing Florida Peninsula, at 84-96th hours - to entering continental part of USA. $R_2$=142 km at 57th hour.

Table 3.

Correlation of the field data on TH WILMA (West North Atlantics)

| TIME | LAT | LON | $R_{64}$ NE | $R_{64}$ SE | $R_{64}$ SW | $R_{64}$ NW | $R_{50}$ NE | $R_{50}$ SE | $R_{50}$ SW | $R_{50}$ NW | $R_{34}$ NE | $R_{34}$ SE | $R_{34}$ SW | $R_{34}$ NW | $\alpha$ | $C_W$ | $C_A$ | Q | $U_{tn}$ | $N_{al}$ |
|---|---|---|---|---|---|---|---|---|---|---|---|---|---|---|---|---|---|---|---|---|
| (h) | (deg) | (deg) | (knmi) | (knmi) | (knmi) | (knmi) | (knmi) | (knmi) | (knmi) | (knmi) | (knmi) | (knmi) | (knmi) | (knmi) | [grad] | | | (kJ $cm^{-2}$) | (knot) | |
| 1 | 2 | 3 | 4 | 5 | 6 | 7 | 8 | 9 | 10 | 11 | 12 | 13 | 14 | 15 | 16 | 17 | 18 | 19 | 20 | 21 |
| -6 | 15.8 | 80.2 | | | | | | | | | | | | | | | | | | |
| 0 | 15.7 | 80.0 | | | | | 20 | 20 | 0 | 20 | 60 | 60 | 30 | 60 | 300 | 1.00 | 1.00 | 75 | 60 | 57.5 |
| 6 | 16.5 | 80.6 | 15 | 15 | 0 | 15 | 30 | 20 | 20 | 30 | 105 | 75 | 50 | 105 | 320 | 1.00 | 1.00 | 80 | 65 | 41.3 |
| 12 | 16.7 | 81.5 | 15 | 15 | 15 | 15 | 50 | 30 | 30 | 50 | 120 | 75 | 60 | 120 | 290 | 1.00 | 1.00 | 90 | 70 | 28.7 |
| 18 | 16.8 | 82.1 | 15 | 15 | 15 | 15 | 60 | 30 | 30 | 60 | 135 | 90 | 90 | 135 | 285 | 1.00 | 1.00 | 90 | **95** | 20.7 |
| 20 | 16.9 | 82.0 | 15 | 15 | 15 | 15 | 60 | 30 | 30 | 60 | 135 | 90 | 90 | 135 | 295 | 1.00 | 1.00 | 90 | **130** | 33.6 |
| 24 | 17.2 | 82.5 | 15 | 15 | 15 | 15 | 60 | 30 | 30 | 60 | 140 | 90 | 90 | 140 | 295 | 1.00 | 1.00 | 90 | 150 | 38.9 |
| 30 | 17.4 | 83.2 | 45 | 20 | 20 | 45 | 70 | 45 | 45 | 70 | 140 | 90 | 90 | 140 | 300 | 1.00 | 1.00 | 100 | 150 | 43.5 |
| 36 | 17.7 | 83.7 | 50 | 40 | 40 | 50 | 75 | 60 | 60 | 75 | 200 | 200 | 100 | 150 | 295 | 1.00 | 1.00 | 100 | 140 | 45.2 |
| 42 | 18.1 | 84.3 | 60 | 40 | 40 | 60 | 75 | 75 | 60 | 75 | 200 | 200 | 110 | 150 | 300 | 1.00 | 1.00 | 90 | 135 | 29.7 |
| 48 | 18.3 | 85.0 | 60 | 40 | 40 | 60 | 75 | 75 | 60 | 75 | 200 | 200 | 110 | 150 | 295 | 1.00 | 1.00 | 85 | 130 | 34.7 |
| 54 | 18.4 | 85.5 | 80 | 75 | 45 | 75 | 110 | 85 | 60 | 110 | 225 | 150 | 110 | 225 | 295 | 1.00 | 1.00 | 85 | 125 | 20.3 |
| 60 | 18.9 | 85.7 | 75 | 75 | 60 | 75 | 110 | 90 | 75 | 110 | 175 | 150 | 120 | 175 | 310 | 1.00 | 1.00 | 90 | 130 | 19.2 |
| 66 | 19.3 | 86.0 | 75 | 75 | 60 | 75 | 110 | 90 | 75 | 110 | 175 | 150 | 120 | 175 | 325 | 1.00 | 1.00 | 95 | 130 | 19.8 |
| 72 | 20.0 | 86.2 | 75 | 75 | 60 | 75 | 110 | 90 | 75 | 110 | 175 | 150 | 120 | 175 | 330 | 1.00 | 0.97 | 95 | 130 | 11.3 |
| 78 | 20.2 | 86.5 | 75 | 75 | 60 | 75 | 100 | 90 | 75 | 100 | 175 | 175 | 120 | 150 | 325 | 0.92 | 0.90 | 90 | 125 | 9.7 |
| 84 | 20.6 | 86.9 | 75 | 75 | 60 | 75 | 100 | 100 | 75 | 100 | 175 | 175 | 120 | 150 | 320 | 0.64 | 0.77 | | 120 | |
| 90 | 20.8 | 86.9 | 75 | 75 | 60 | 75 | 100 | 100 | 75 | 100 | 175 | 175 | 120 | 150 | 330 | 0.64 | 0.79 | | 120 | |
| 96 | 20.9 | 87.2 | 75 | 75 | 60 | 75 | 100 | 100 | 75 | 100 | 175 | 175 | 120 | 150 | 300 | 0.62 | 0.77 | | 110 | |
| 102 | 21.3 | 87.0 | 75 | 75 | 60 | 75 | 100 | 100 | 75 | 100 | 175 | 175 | 120 | 150 | 0 | 0.65 | 0.79 | | 100 | |
| 108 | 21.4 | 87.1 | 75 | 75 | 50 | 75 | 120 | 100 | 75 | 100 | 175 | 175 | 120 | 150 | 0 | 0.63 | 0.79 | | 85 | |
| 114 | 21.8 | 86.9 | 60 | 60 | 50 | 60 | 100 | 90 | 75 | 90 | 175 | 175 | 120 | 150 | 10 | 0.62 | 0.81 | | 85 | |
| 120 | 22.1 | 86.6 | 60 | 60 | 40 | 40 | 100 | 100 | 75 | 90 | 175 | 175 | 125 | 175 | 45 | 0.62 | 0.85 | | 85 | |
| 126 | 22.7 | 85.8 | 60 | 60 | 40 | 40 | 100 | 100 | 75 | 90 | 175 | 175 | 125 | 175 | 45 | 0.71 | 0.93 | 80 | 85 | 34.0 |
| 132 | 23.5 | 84.9 | 65 | 75 | 50 | 50 | 125 | 125 | 90 | 90 | 200 | 200 | 150 | 150 | 45 | 0.88 | 0.96 | 70 | 90 | 25.7 |
| 138 | 24.4 | 83.7 | 65 | 75 | 50 | 50 | 125 | 125 | 90 | 90 | 200 | 200 | 150 | 150 | 50 | 1.00 | 0.92 | 55 | 100 | 23.4 |
| 144 | 25.5 | 82.4 | 75 | 80 | 75 | 50 | 125 | 125 | 125 | 90 | 200 | 200 | 175 | 150 | 50 | 0.91 | 0.76 | 45 | 110 | 17.3 |
| 150 | 26.9 | 80.0 | 75 | 85 | 75 | 50 | 125 | 125 | 100 | 90 | 200 | 225 | 200 | 150 | 45 | 1.00 | 0.79 | 50 | 90 | 25.4 |
| 153.5 | 28.1 | 78.8 | 75 | 90 | 75 | 40 | 125 | 150 | 100 | 90 | 200 | 225 | 200 | 150 | 45 | 0.30 | 0.81 | | 100 | |

| 1 | 2 | 3 | 4 | 5 | 6 | 7 | 8 | 9 | 10 | 11 | 12 | 13 | 14 | 15 | 16 | 17 | 18 | 19 | 20 | 21 |
|---|---|---|---|---|---|---|---|---|---|---|---|---|---|---|---|---|---|---|---|---|
| 156 | 29.0 | 77.4 | 75 | 90 | 75 | 40 | 125 | 150 | 100 | 90 | 200 | 225 | 200 | 150 | 45 | 0.60 | 0.94 | | 105 | |
| 162 | 31.6 | 74.3 | 75 | 90 | 75 | 40 | 125 | 150 | 100 | 90 | 200 | 225 | 200 | 150 | 45 | 1.00 | 1.00 | 30 | 110 | 23.0 |
| 168 | 34.8 | 70.0 | 75 | 90 | 60 | 20 | 125 | 150 | 100 | 40 | 150 | 275 | 375 | 100 | 50 | 1.00 | 1.00 | 20 | 100 | 13.9 |
| 174 | 34.8 | 70.0 | | | | | | | | | | | | | | | | | | |

The point 0 corresponds to 21:00 UT, September 19, 2005. Rapid intensification (with intensification rate 17.5 knot/h) is observed at 18-20th hours. Blank spaces at 84-120th hours correspond to covering of Yucatan Peninsula, at 153-156th hours - to crossing Florida Peninsula. $R_2$=88 km at 20th hour.

Table 4.

Correlation of the field data on super typhoon DIAMNU (North West Pacific)

| TIME | LAT | LON | $R_{64}$ NE | $R_{64}$ SE | $R_{64}$ SW | $R_{64}$ NW | $R_{50}$ NE | $R_{50}$ SE | $R_{50}$ SW | $R_{50}$ NW | $R_{34}$ NE | $R_{34}$ SE | $R_{34}$ SW | $R_{34}$ NW | $\alpha$ | $C_W$ | $C_A$ | Q | $U_{tn}$ | $N_{al}$ |
|---|---|---|---|---|---|---|---|---|---|---|---|---|---|---|---|---|---|---|---|---|
| (h) | (deg) | (deg) | (knmi) | (knmi) | (knmi) | (knmi) | (knmi) | (knmi) | (knmi) | (knmi) | (knmi) | (knmi) | (knmi) | (knmi) | [grad] | | | (kJ $cm^{-2}$) | (knot) | |
| -6 | 9.8 | 137.0 | | | | | | | | | | | | | | | | | | |
| 0 | 10.7 | 137.4 | 20 | 20 | 20 | 20 | 25 | 25 | 30 | 25 | 100 | 100 | 110 | 100 | 25 | 1.00 | 1.00 | 80 | 65 | 48.0 |
| 6 | 11.2 | 137.5 | 20 | 20 | 20 | 20 | 25 | 25 | 30 | 25 | 100 | 100 | 110 | 100 | 10 | 1.00 | 1.00 | 85 | 70 | 40.8 |
| 12 | 11.9 | 137.2 | 20 | 20 | 20 | 20 | 25 | 25 | 30 | 25 | 105 | 105 | 115 | 105 | 350 | 1.00 | 1.00 | 90 | **85** | 32.7 |
| 18 | 12.7 | 136.9 | 35 | 35 | 35 | 35 | 50 | 50 | 60 | 50 | 140 | 140 | 160 | 140 | 340 | 1.00 | 1.00 | 95 | **120** | 27.0 |
| 24 | 13.4 | 136.8 | 35 | 35 | 35 | 35 | 70 | 70 | 75 | 70 | 130 | 140 | 130 | 130 | 350 | 1.00 | 1.00 | 95 | 145 | 34.9 |
| 30 | 14.3 | 136.6 | 40 | 40 | 40 | 40 | 75 | 75 | 75 | 75 | 145 | 140 | 140 | 130 | 350 | 1.00 | 1.00 | 95 | 150 | 37.0 |
| 36 | 15.1 | 136.0 | 40 | 40 | 40 | 40 | 70 | 75 | 70 | 70 | 140 | 150 | 140 | 140 | 325 | 1.00 | 1.00 | 100 | 155 | 35.2 |
| 42 | 15.7 | 135.6 | 40 | 40 | 40 | 40 | 70 | 75 | 70 | 70 | 140 | 150 | 140 | 140 | 325 | 1.00 | 1.00 | 100 | 155 | 30.3 |
| 48 | 16.5 | 135.2 | 40 | 40 | 40 | 40 | 70 | 75 | 70 | 70 | 140 | 150 | 140 | 140 | 330 | 1.00 | 1.00 | 90 | 155 | 27.3 |
| 54 | 17.1 | 134.8 | 40 | 40 | 40 | 40 | 70 | 75 | 70 | 70 | 140 | 150 | 140 | 140 | 330 | 1.00 | 1.00 | 85 | 155 | 31.0 |
| 60 | 17.6 | 133.8 | 40 | 40 | 40 | 40 | 70 | 70 | 60 | 60 | 150 | 150 | 150 | 150 | 305 | 1.00 | 1.00 | 90 | 140 | 38.7 |
| 66 | 17.9 | 132.8 | 60 | 60 | 60 | 60 | 90 | 90 | 90 | 90 | 150 | 150 | 170 | 170 | 295 | 1.00 | 1.00 | 85 | 130 | 23.0 |
| 72 | 18.0 | 132.1 | 70 | 70 | 70 | 70 | 90 | 120 | 120 | 90 | 150 | 150 | 170 | 170 | 285 | 1.00 | 1.00 | 80 | 125 | 21.8 |
| 78 | 18.4 | 131.8 | 70 | 70 | 70 | 70 | 100 | 100 | 100 | 100 | 150 | 150 | 170 | 170 | 315 | 1.00 | 1.00 | 75 | 115 | 25.7 |
| 84 | 19.3 | 131.3 | 70 | 70 | 70 | 70 | 100 | 100 | 100 | 100 | 150 | 150 | 160 | 170 | 330 | 1.00 | 1.00 | 70 | 120 | 24.6 |
| 90 | 20.3 | 130.4 | 70 | 70 | 70 | 70 | 100 | 100 | 100 | 100 | 150 | 150 | 160 | 170 | 326 | 1.00 | 1.00 | 60 | 125 | 19.4 |
| 96 | 21.2 | 129.7 | 70 | 70 | 70 | 70 | 100 | 100 | 100 | 100 | 160 | 160 | 180 | 180 | 325 | 1.00 | 1.00 | 55 | 125 | 13.2 |
| 102 | 22.4 | 129.3 | 70 | 70 | 50 | 50 | 150 | 150 | 120 | 120 | 220 | 220 | 180 | 180 | 340 | 1.00 | 1.00 | 45 | 125 | 10.7 |
| 108 | 23.3 | 129.1 | 50 | 50 | 50 | 50 | 120 | 150 | 80 | 80 | 200 | 220 | 180 | 180 | 350 | 1.00 | 1.00 | 40 | 120 | 15.3 |
| 114 | 24.4 | 129.2 | 40 | 40 | 40 | 40 | 120 | 100 | 100 | 100 | 220 | 200 | 180 | 180 | 5 | 1.00 | 1.00 | 35 | 105 | 15.0 |
| 120 | 25.6 | 129.3 | 40 | 40 | 40 | 30 | 120 | 100 | 100 | 50 | 200 | 200 | 180 | 120 | 10 | 1.00 | 1.00 | 30 | 90 | 13.1 |
| 126 | 26.9 | 129.7 | 40 | 40 | 40 | 30 | 100 | 120 | 80 | 50 | 180 | 200 | 180 | 120 | 15 | 1.00 | 1.00 | 25 | 80 | 12.3 |
| 132 | 28.0 | 130.4 | 30 | 20 | 20 | 20 | 90 | 90 | 70 | 40 | 200 | 200 | 180 | 120 | 30 | 1.00 | 0.99 | 20 | 70 | 12.0 |
| 138 | 29.5 | 131.3 | 0 | 0 | 0 | 0 | 80 | 80 | 60 | 60 | 180 | 180 | 160 | 160 | 30 | 1.00 | 0.96 | 15 | 70 | 14.6 |
| 144 | 31.0 | 132.1 | | | | | | | | | | | | | | | | | | |

The point 0 corresponds to 18:00 UT, June 14, 2004. Rapid intensification (with intensification factor 17.5 knot/h) is observed at 12-18th hours. $R_2$=98 km at 18th hour.

Table 5.

Correlation of the field data on super typhoon CHABA (North West Pacific)

| TIME | LAT | LON | $R_{64}$ NE | $R_{64}$ SE | $R_{64}$ SW | $R_{64}$ NW | $R_{50}$ NE | $R_{50}$ SE | $R_{50}$ SW | $R_{50}$ NW | $R_{34}$ NE | $R_{34}$ SE | $R_{34}$ SW | $R_{34}$ NW | $\alpha$ | $C_W$ | $C_A$ | Q | $U_{tn}$ | $N_{al}$ |
|---|---|---|---|---|---|---|---|---|---|---|---|---|---|---|---|---|---|---|---|---|
| (h) | (deg) | (deg) | (knmi) | (knmi) | (knmi) | (knmi) | (knmi) | (knmi) | (knmi) | (knmi) | (knmi) | (knmi) | (knmi) | (knmi) | [grad] | | | (kJ $cm^{-2}$) | (knot) | |
| 1 | 2 | 3 | 4 | 5 | 6 | 7 | 8 | 9 | 10 | 11 | 12 | 13 | 14 | 15 | 16 | 17 | 18 | 19 | 20 | 21 |
| -6 | 13.7 | 158.0 | | | | | | | | | | | | | | | | | | |
| 0 | 14.5 | 157.0 | 0 | 0 | 0 | 0 | 10 | 10 | 10 | 10 | 75 | 80 | 80 | 85 | 300 | 1.00 | 1.00 | 115 | 60 | 127.8 |
| 6 | 14.6 | 155.4 | 0 | 0 | 0 | 0 | 15 | 15 | 15 | 15 | 90 | 90 | 90 | 85 | 280 | 1.00 | 1.00 | 115 | 65 | 122.3 |
| 12 | 14.8 | 154.1 | 0 | 0 | 0 | 0 | 15 | 15 | 15 | 15 | 90 | 90 | 90 | 90 | 280 | 1.00 | 1.00 | 110 | 65 | 102.4 |
| 18 | 14.7 | 153.2 | 10 | 10 | 10 | 10 | 30 | 30 | 30 | 30 | 70 | 90 | 90 | 70 | 270 | 1.00 | 1.00 | 100 | 70 | 72.1 |
| 24 | 14.3 | 151.9 | 10 | 10 | 10 | 10 | 40 | 40 | 40 | 40 | 110 | 125 | 125 | 110 | 265 | 1.00 | 1.00 | 90 | 70 | 56.6 |
| 30 | 14.1 | 150.3 | 20 | 20 | 20 | 20 | 40 | 45 | 45 | 40 | 110 | 140 | 140 | 110 | 265 | 1.00 | 1.00 | 85 | 75 | 60.2 |
| 36 | 14.4 | 148.8 | 20 | 30 | 30 | 20 | 50 | 60 | 60 | 50 | 120 | 160 | 160 | 120 | 280 | 1.00 | 1.00 | 85 | 90 | 49.0 |
| 42 | 14.0 | 147.4 | 30 | 40 | 40 | 30 | 60 | 80 | 80 | 60 | 140 | 170 | 170 | 140 | 260 | 1.00 | 1.00 | 90 | 95 | 44.8 |
| 48 | 14.4 | 146.3 | 35 | 45 | 45 | 35 | 50 | 80 | 80 | 50 | 140 | 180 | 180 | 140 | 285 | 1.00 | 1.00 | 90 | 110 | 39.6 |
| 54 | 14.4 | 145.4 | 40 | 50 | 50 | 40 | 60 | 90 | 90 | 60 | 140 | 180 | 180 | 140 | 270 | 1.00 | 1.00 | 85 | **125** | 32.7 |
| 60 | 14.8 | 144.8 | 30 | 50 | 50 | 30 | 75 | 90 | 90 | 75 | 180 | 200 | 200 | 180 | 295 | 1.00 | 1.00 | 85 | **155** | 31.9 |
| 66 | 15.2 | 143.6 | 30 | 50 | 50 | 30 | 75 | 90 | 90 | 75 | 180 | 200 | 200 | 180 | 285 | 1.00 | 1.00 | 85 | 155 | 30.3 |
| 72 | 15.6 | 142.9 | 30 | 50 | 50 | 30 | 75 | 90 | 90 | 75 | 180 | 220 | 220 | 180 | 300 | 1.00 | 1.00 | 80 | 155 | 25.8 |
| 78 | 16.3 | 142.1 | 40 | 60 | 60 | 40 | 80 | 120 | 120 | 80 | 160 | 210 | 210 | 160 | 310 | 1.00 | 1.00 | 75 | 155 | 26.1 |
| 84 | 16.9 | 141.2 | 40 | 60 | 60 | 40 | 80 | 120 | 120 | 80 | 160 | 200 | 220 | 160 | 310 | 1.00 | 1.00 | 70 | 150 | 25.0 |
| 90 | 17.4 | 140.2 | 40 | 60 | 60 | 40 | 80 | 120 | 120 | 80 | 160 | 200 | 220 | 160 | 300 | 1.00 | 1.00 | 65 | 150 | 19.8 |
| 96 | 18.0 | 139.6 | 40 | 60 | 60 | 40 | 80 | 120 | 120 | 80 | 160 | 220 | 200 | 160 | 315 | 1.00 | 1.00 | 60 | 150 | 15.8 |
| 102 | 18.5 | 139.1 | 40 | 60 | 60 | 40 | 80 | 120 | 120 | 80 | 160 | 200 | 200 | 160 | 315 | 1.00 | 1.00 | 55 | 140 | 19.3 |
| 108 | 19.4 | 138.7 | 40 | 60 | 60 | 40 | 80 | 120 | 120 | 80 | 160 | 200 | 200 | 160 | 335 | 1.00 | 1.00 | 55 | 150 | 19.3 |
| 114 | 20.3 | 138.2 | 40 | 40 | 40 | 40 | 60 | 80 | 80 | 60 | 130 | 200 | 200 | 130 | 330 | 1.00 | 1.00 | 50 | 150 | 18.2 |
| 120 | 21.2 | 137.6 | 40 | 40 | 40 | 40 | 60 | 80 | 80 | 60 | 130 | 200 | 200 | 130 | 330 | 1.00 | 1.00 | 50 | 145 | 17.2 |
| 126 | 22.0 | 137.1 | 40 | 40 | 40 | 40 | 80 | 90 | 90 | 80 | 160 | 200 | 200 | 160 | 330 | 1.00 | 1.00 | 50 | 145 | 14.4 |
| 132 | 22.7 | 136.6 | 40 | 40 | 40 | 40 | 80 | 90 | 90 | 80 | 170 | 200 | 200 | 170 | 330 | 1.00 | 1.00 | 50 | 145 | 15.8 |
| 138 | 23.4 | 136.2 | 40 | 40 | 40 | 40 | 80 | 90 | 90 | 80 | 150 | 180 | 180 | 170 | 330 | 1.00 | 1.00 | 50 | 140 | 15.3 |
| 150 | 24.8 | 135.2 | 50 | 50 | 45 | 45 | 90 | 90 | 70 | 70 | 200 | 200 | 170 | 170 | 325 | 1.00 | 1.00 | 45 | 115 | 18.9 |
| 156 | 25.7 | 135.1 | 50 | 50 | 50 | 50 | 90 | 90 | 70 | 70 | 150 | 150 | 130 | 130 | 345 | 1.00 | 1.00 | 45 | 110 | 20.8 |
| 162 | 26.1 | 134.9 | 50 | 50 | 50 | 50 | 90 | 90 | 65 | 65 | 150 | 150 | 125 | 125 | 335 | 1.00 | 1.00 | 45 | 105 | 11.0 |
| 168 | 26.6 | 134.5 | 50 | 50 | 50 | 50 | 90 | 90 | 65 | 65 | 150 | 150 | 125 | 125 | 325 | 1.00 | 1.00 | 45 | 100 | 8.8 |

| 1 | 2 | 3 | 4 | 5 | 6 | 7 | 8 | 9 | 10 | 11 | 12 | 13 | 14 | 15 | 16 | 17 | 18 | 19 | 20 | 21 |
|---|---|---|---|---|---|---|---|---|---|---|---|---|---|---|---|---|---|---|---|---|
| 174 | 26.8 | 134.3 | 50 | 50 | 50 | 50 | 90 | 90 | 80 | 80 | 180 | 180 | 130 | 130 | 320 | 1.00 | 1.00 | 45 | 100 | 9.0 |
| 180 | 27.1 | 134.2 | 50 | 50 | 50 | 50 | 100 | 90 | 90 | 90 | 200 | 180 | 130 | 130 | 335 | 1.00 | 1.00 | 50 | 115 | 20.0 |
| 186 | 27.2 | 133.8 | 60 | 60 | 60 | 60 | 130 | 110 | 80 | 80 | 220 | 220 | 180 | 180 | 305 | 1.00 | 1.00 | 50 | 115 | 20.5 |
| 192 | 27.3 | 133.6 | 80 | 60 | 60 | 60 | 100 | 80 | 80 | 80 | 220 | 140 | 140 | 200 | 300 | 1.00 | 1.00 | 50 | 115 | 12.1 |
| 198 | 27.7 | 132.7 | 80 | 60 | 60 | 60 | 100 | 80 | 80 | 80 | 220 | 200 | 180 | 200 | 295 | 1.00 | 1.00 | 50 | 110 | 7.0 |
| 204 | 27.8 | 132.1 | 70 | 60 | 60 | 60 | 90 | 80 | 80 | 80 | 220 | 200 | 200 | 180 | 285 | 1.00 | 1.00 | 55 | 110 | 15.7 |
| 210 | 28.2 | 131.3 | 70 | 60 | 60 | 60 | 90 | 80 | 80 | 80 | 220 | 200 | 190 | 180 | 300 | 1.00 | 1.00 | 55 | 105 | 23.2 |
| 216 | 28.8 | 130.5 | 50 | 50 | 50 | 50 | 80 | 80 | 80 | 80 | 200 | 180 | 180 | 180 | 315 | 1.00 | 1.00 | 55 | 100 | 22.8 |
| 222 | 29.4 | 130.0 | 50 | 50 | 50 | 50 | 80 | 80 | 80 | 80 | 200 | 180 | 180 | 180 | 325 | 1.00 | 0.97 | 55 | 95 | 17.7 |
| 228 | 30.2 | 129.7 | 50 | 50 | 50 | 50 | 85 | 85 | 85 | 85 | 200 | 180 | 180 | 180 | 340 | 1.00 | 0.96 | 60 | 90 | 31.8 |
| 234 | 31.5 | 130.2 | 50 | 50 | 50 | 50 | 80 | 80 | 80 | 80 | 180 | 170 | 160 | 160 | 20 | 1.00 | 0.93 | 65 | 85 | 54.7 |
| 240 | 33.3 | 131.3 | 40 | 40 | 40 | 40 | 60 | 60 | 60 | 60 | 180 | 140 | 110 | 110 | 25 | 1.00 | 0.79 | 65 | 80 | 77.0 |
| 246 | 35.0 | 133.0 | 40 |  |  |  |  |  |  |  |  |  |  |  |  |  |  |  |  |  |

The point 0 corresponds to 06:00 UT, August 20, 2004. Rapid intensification (with intensification rate 5.0 knot/h) is observed at 54-60th hours. $R_2$=154 km at 18th hour.

Table 6.

Correlation of the field data on cyclone NANCY (South Pacific)

| TIME | LAT | LON | $R_{64}$ NE | $R_{64}$ SE | $R_{64}$ SW | $R_{64}$ NW | $R_{50}$ NE | $R_{50}$ SE | $R_{50}$ SW | $R_{50}$ NW | $R_{34}$ NE | $R_{34}$ SE | $R_{34}$ SW | $R_{34}$ NW | $\alpha$ | $C_W$ | $C_A$ | Q | $U_{tn}$ | $N_{al}$ |
|---|---|---|---|---|---|---|---|---|---|---|---|---|---|---|---|---|---|---|---|---|
| (h) | (deg) | (deg) | (knmi) | (knmi) | (knmi) | (knmi) | (knmi) | (knmi) | (knmi) | (knmi) | (knmi) | (knmi) | (knmi) | (knmi) | [grad] | | | (kJ $cm^{-2}$) | (knot) | |
| 0 | 13.6 | 164.2 | 0 | 0 | 0 | 0 | 0 | 0 | 0 | 0 | 50 | 60 | 60 | 50 | 165 | 1.00 | 1.00 | 85 | **45** | **31.3** |
| 12 | 14.0 | 163.5 | 30 | 30 | 30 | 30 | 60 | 60 | 60 | 60 | 100 | 120 | 120 | 100 | 125 | 1.00 | 1.00 | 80 | **120** | **34.7** |
| 24 | 15.3 | 160.9 | 30 | 30 | 30 | 30 | 60 | 60 | 60 | 60 | 100 | 120 | 120 | 100 | 125 | 1.00 | 1.00 | 75 | 125 | 55.3 |
| 42 | 19.2 | 158.7 | 30 | 30 | 25 | 25 | 50 | 50 | 25 | 25 | 120 | 120 | 100 | 100 | 170 | 1.00 | 1.00 | 50 | 95 | 41.2 |
| 48 | 20.3 | 158.3 | 25 | 25 | 25 | 25 | 40 | 40 | 25 | 25 | 110 | 110 | 90 | 90 | 165 | 1.00 | 1.00 | 45 | 90 | 37.7 |
| 60 | 22.0 | 159.9 | 0 | 0 | 0 | 0 | 30 | 30 | 30 | 30 | 80 | 100 | 100 | 80 | 165 | 1.00 | 1.00 | 40 | 65 | 37.1 |

The point 0 corresponds to 18:00 UT, February 13, 2005. Rapid intensification (with intensification rate 5.0 knot/h) is observed at 0-12th hours. $R_2$=111 km at 12th hour. In connection with small number of positions TH back boundary translation speeds at 0 and 60 hours are determines through equations (17) and (16), respectively.

Table 7.

Correlation of the field data on cyclone OLAF (South Pacific)

| TIME | LAT | LON | $R_{64}$ | $R_{64}$ | $R_{64}$ | $R_{64}$ | $R_{50}$ | $R_{50}$ | $R_{50}$ | $R_{50}$ | $R_{34}$ | $R_{34}$ | $R_{34}$ | $R_{34}$ | $\alpha$ | $C_W$ | $C_A$ | Q | $U_{tn}$ | $N_{al}$ |
|---|---|---|---|---|---|---|---|---|---|---|---|---|---|---|---|---|---|---|---|---|
| | | | NE | SE | SW | NW | NE | SE | SW | NW | NE | SE | SW | NW | | | | | | |
| (h) | (deg) | (deg) | (knmi) | (knmi) | (knmi) | (knmi) | (knmi) | (knmi) | (knmi) | (knmi) | (knmi) | (knmi) | (knmi) | (knmi) | [grad] | | | (kJ $cm^{-2}$) | (knot) | |
| -6 | 9.6 | 177.4 | | | | | | | | | | | | | | | | | | |
| 0 | 9.4 | 178.0 | 15 | 15 | 15 | 15 | 25 | 25 | 25 | 25 | 80 | 90 | 90 | 80 | 285 | 1.00 | 1.00 | 140 | 70 | 254.8 |
| 6 | 9.2 | 177.9 | 15 | 15 | 15 | 15 | 30 | 30 | 30 | 30 | 80 | 90 | 90 | 80 | 0 | 1.00 | 1.00 | 135 | 90 | 238.9 |
| 12 | 9.4 | 177.1 | 15 | 15 | 15 | 15 | 30 | 30 | 30 | 30 | 80 | 90 | 90 | 80 | 110 | 1.00 | 1.00 | 130 | **90** | 208.7 |
| 18 | 9.8 | 175.9 | 20 | 20 | 20 | 20 | 30 | 30 | 30 | 30 | 80 | 90 | 90 | 80 | 105 | 1.00 | 1.00 | 125 | **125** | 91.0 |
| 24 | 10.7 | 175.1 | 20 | 20 | 20 | 20 | 30 | 30 | 30 | 30 | 85 | 95 | 95 | 85 | 130 | 1.00 | 1.00 | 120 | 125 | 65.1 |
| 30 | 11.5 | 174.5 | 20 | 20 | 20 | 20 | 30 | 30 | 30 | 30 | 80 | 90 | 90 | 80 | 135 | 1.00 | 1.00 | 125 | 125 | 65.2 |
| 36 | 12.0 | 174.1 | 25 | 25 | 25 | 25 | 35 | 35 | 35 | 35 | 95 | 85 | 85 | 95 | 140 | 1.00 | 1.00 | 125 | 120 | 72.6 |
| 42 | 12.2 | 173.6 | 25 | 25 | 25 | 25 | 40 | 40 | 40 | 40 | 115 | 105 | 105 | 115 | 120 | 1.00 | 1.00 | 125 | 135 | 97.3 |
| 48 | 12.2 | 172.6 | 25 | 25 | 25 | 25 | 45 | 45 | 45 | 45 | 120 | 105 | 120 | 120 | 95 | 1.00 | 1.00 | 125 | 140 | 79.3 |
| 54 | 12.6 | 171.3 | 35 | 35 | 35 | 35 | 45 | 45 | 45 | 45 | 95 | 110 | 110 | 95 | 110 | 1.00 | 1.00 | 130 | 145 | 67.7 |
| 60 | 13.3 | 170.1 | 35 | 35 | 35 | 35 | 45 | 45 | 45 | 45 | 100 | 120 | 120 | 100 | 120 | 1.00 | 1.00 | 135 | 145 | 68.4 |
| 66 | 14.4 | 169.2 | 20 | 20 | 20 | 20 | 40 | 40 | 40 | 40 | 95 | 105 | 105 | 95 | 140 | 1.00 | 1.00 | 125 | 140 | 93.0 |
| 72 | 15.4 | 168.2 | 25 | 25 | 25 | 25 | 40 | 40 | 40 | 40 | 95 | 105 | 105 | 95 | 135 | 1.00 | 1.00 | 130 | 140 | 97.6 |
| 78 | 16.3 | 167.3 | 25 | 25 | 25 | 25 | 40 | 40 | 40 | 40 | 95 | 105 | 105 | 95 | 145 | 1.00 | 1.00 | 120 | 130 | 85.9 |
| 90 | 18.5 | 165.7 | 25 | 25 | 25 | 25 | 45 | 40 | 40 | 45 | 115 | 105 | 105 | 115 | 140 | 1.00 | 1.00 | 70 | 120 | 65.5 |
| 102 | 21.2 | 162.9 | 25 | 25 | 25 | 25 | 45 | 40 | 40 | 45 | 120 | 110 | 110 | 120 | 140 | 1.00 | 1.00 | 50 | 115 | 51.2 |
| 114 | 24.9 | 160.8 | 40 | 40 | 40 | 40 | 60 | 50 | 50 | 60 | 120 | 140 | 120 | 140 | 155 | 1.00 | 1.00 | 25 | 90 | 19.9 |
| 126 | 28.0 | 160.6 | 0 | 0 | 0 | 0 | 35 | 35 | 25 | 25 | 105 | 105 | 105 | 110 | 175 | 1.00 | 1.00 | 15 | 65 | 17.2 |
| 138 | 30.7 | 161.3 | | | | | | | | | | | | | | | | | | |

The point 0 corresponds to 00:00 UT, February 14, 2005. Rapid intensification (with intensification rate 5.83 knot/h) is observed at 12-18th hours. $R_2$=56 km at 18th hour.

Table 8.

Correlation of the field data on cyclone INGRID (South Pacific and South Indian)

| TIME | LAT | LON | $R_{64}$ NE | $R_{64}$ SE | $R_{64}$ SW | $R_{64}$ NW | $R_{50}$ NE | $R_{50}$ SE | $R_{50}$ SW | $R_{50}$ NW | $R_{34}$ NE | $R_{34}$ SE | $R_{34}$ SW | $R_{34}$ NW | $\alpha$ | $C_W$ | $C_A$ | Q | $U_{tn}$ | $N_{al}$ |
|---|---|---|---|---|---|---|---|---|---|---|---|---|---|---|---|---|---|---|---|---|
| (h) | (deg) | (deg) | (knmi) | (knmi) | (knmi) | (knmi) | (knmi) | (knmi) | (knmi) | (knmi) | (knmi) | (knmi) | (knmi) | (knmi) | [grad] | | | (kJ $cm^{-2}$) | (knot) | |
| -12 | 13.2 | 148.3 | | | | | | | | | | | | | | | | | | |
| 0 | 13.7 | 149.0 | 15 | 15 | 15 | 15 | 45 | 45 | 40 | 45 | 110 | 110 | 110 | 110 | 115 | 1.00 | 1.00 | 50 | 75 | 26.1 |
| 12 | 14.2 | 148.6 | 25 | 25 | 25 | 25 | 55 | 55 | 45 | 50 | 105 | 95 | 80 | 90 | 245 | 1.00 | 1.00 | 50 | 120 | 33.8 |
| 24 | 13.9 | 148.0 | 25 | 25 | 25 | 25 | 45 | 45 | 45 | 45 | 100 | 100 | 100 | 100 | 305 | 1.00 | 1.00 | 55 | 130 | 23.8 |
| 36 | 13.9 | 146.9 | 35 | 35 | 35 | 35 | 45 | 45 | 45 | 45 | 90 | 90 | 90 | 90 | 270 | 1.00 | 1.00 | 50 | 130 | 16.5 |
| 48 | 13.8 | 146.0 | 20 | 20 | 20 | 20 | 35 | 35 | 35 | 35 | 85 | 85 | 80 | 85 | 280 | 1.00 | 0.93 | 45 | 105 | 16.0 |
| 60 | 13.6 | 145.0 | 20 | 20 | 20 | 20 | 35 | 35 | 35 | 35 | 85 | 85 | 75 | 85 | 270 | 1.00 | 0.89 | 40 | 105 | 16.4 |
| 72 | 13.2 | 143.7 | 25 | 25 | 25 | 25 | 35 | 35 | 35 | 35 | 80 | 80 | 70 | 70 | 285 | 1.00 | 0.48 | | 100 | |
| 84 | 13.5 | 141.7 | 0 | 0 | 0 | 0 | 30 | 30 | 30 | 30 | 60 | 60 | 60 | 60 | 255 | 0.35 | 0.51 | | 65 | |
| 108 | 12.3 | 138.7 | 10 | 10 | 10 | 10 | 20 | 20 | 20 | 20 | 60 | 70 | 70 | 70 | 290 | 1.00 | 1.00 | 45 | **80** | **32.5** |
| 114 | 12.2 | 137.8 | 25 | 25 | 20 | 30 | 40 | 40 | 25 | 45 | 80 | 80 | 65 | 90 | 275 | 1.00 | 0.98 | 40 | **120** | **23.6** |
| 120 | 11.9 | 136.8 | 25 | 25 | 20 | 30 | 40 | 40 | 25 | 45 | 80 | 80 | 65 | 90 | 280 | 1.00 | 0.84 | 40 | 120 | 24.2 |
| 132 | 11.6 | 134.9 | 25 | 20 | 20 | 30 | 35 | 25 | 25 | 45 | 70 | 65 | 65 | 90 | 275 | 1.00 | 0.80 | 40 | 135 | 25.1 |
| 144 | 11.3 | 132.6 | 25 | 25 | 25 | 25 | 35 | 35 | 35 | 35 | 80 | 65 | 65 | 80 | 275 | 0.69 | 0.93 | 45 | 120 | 41.9 |
| 156 | 11.4 | 131.1 | 25 | 25 | 25 | 25 | 35 | 35 | 35 | 35 | 80 | 65 | 65 | 80 | 255 | 0.77 | 0.91 | 40 | 100 | 22.9 |
| 168 | 11.6 | 130.2 | 25 | 25 | 25 | 25 | 35 | 35 | 35 | 35 | 80 | 55 | 55 | 80 | 250 | 0.75 | 0.93 | 40 | 100 | 19.5 |
| 180 | 11.7 | 129.2 | 25 | 25 | 25 | 25 | 35 | 35 | 35 | 35 | 80 | 55 | 55 | 80 | 255 | 0.85 | 0.98 | 60 | 100 | 24.1 |
| 192 | 12.3 | 128.3 | 25 | 25 | 25 | 25 | 35 | 35 | 35 | 35 | 100 | 65 | 65 | 100 | 235 | 1.00 | 1.00 | 70 | 115 | 21.4 |
| 204 | 13.2 | 127.5 | 35 | 35 | 35 | 35 | 50 | 40 | 40 | 50 | 105 | 85 | 85 | 105 | 230 | 1.00 | 0.97 | 55 | 130 | 18.2 |
| 216 | 14.5 | 126.8 | 35 | 35 | 35 | 35 | 50 | 40 | 40 | 50 | 105 | 85 | 85 | 105 | 210 | 0.63 | 0.48 | | 90 | |
| 228 | 15.5 | 126.4 | 35 | 35 | 35 | 35 | 50 | 40 | 40 | 50 | 105 | 85 | 85 | 105 | 170 | 0.37 | 0.30 | | 75 | |
| 240 | 16.2 | 126.5 | | | | | | | | | | | | | | | | | | |

The point 0 corresponds to 18:00 UT, March 06, 2005. Rapid intensification (with intensification rate 6.67 knot/h) is observed at 108-114th hours. Blank spaces at 72-84th hours correspond to crossing Cape Peninsula, at 216-218th hours - to covering of north coast of Australia. $R_2$=71km at 114th hour.